Ionics (2024) 30:647–675
https://doi.org/10.1007/s11581-023-05318-y

REVIEW

The significance of fillers in composite polymer electrolytes for optimizing lithium battery

Mohan Jagan[1] · **S. P. Vijayachamundeeswari**[1]

Received: 4 July 2023 / Revised: 7 November 2023 / Accepted: 21 November 2023 / Published online: 1 December 2023

Abstract
Solid polymer electrolytes constructed from polymers have high safety, outstanding thermal stability, and minimal flammability as their merits. Many researchers have been working on creating high-performance Li-based batteries composed of solid polymers. Composite polymer electrolyte (CPEs) electrochemical characteristics, which might include conductivity of ions, ion transfer numbers, and electrochemical durability, play an essential role when assessing the performance of energy conservation and conversion systems. Inorganic additions may enhance ionic conductivity by producing an ion transport percolation network. Additionally, the most effective filler composition can improve CPE electrochemical process stability, diminishing adverse responses and deterioration throughout gadget operations. In this article, we talk about active filler-based composites of polymers that make excellent solid electrolytes for the large-scale production of solid-state battery packs. We review the analysis and performance of active filler-based composite polymer electrolytes and look into the design of high-performance composite electrolytes.

Keywords Garnet · Perovskite · Sulfide · Nasicon · Active fillers

Introduction

The exploration of alternative polymer-composite substances for electrolytes or separators for lithium-ion and lithium-based batteries has increased exponentially in the twenty-first century [1]. In recent times, due to their exceptional characteristics, including a high density of energy [2], lightweight [3], extended cycle life [4], flexible morphologies, and minimal leakage, polymeric lithium-ion batteries, as well as all micro-batteries, are considered to be the most prospective recharging chemical source of power [5, 6]. An electrolyte is an essential component in the battery that permits ions to travel between two electrodes, allowing electrical current to flow over the battery to generate and store energy. Rechargeable batteries are composed of electrodes (a cathode and an anode) separated by an electrolyte. Between the charging and discharging cycles, the electrolyte is in a state of charge, transmitting ions between the two electrodes. The terminology "polymer" comes derived from the Greek poly, indicating "many," while Mer indicates "part." The electrolyte is often the solution of acid, base, or salt. Compared to the liquid electrolyte, polymer electrolyte is much more flexible and lightweight. There are a few various electrochemical windows. Its limited conductivity at low temperatures is the primary drawback for polymer electrolytes [7]. Since the previous two decades, polymer electrolytes (PEs) have sparked substantial attention due to their potential usage in solid-state batteries, fuel cells, sensors, super-capacitors, etc. [8–11]. Li-based rechargeable battery polymer electrolytes could generally be split into three primary classifications: composite polymer electrolytes (CPEs), gel polymer electrolytes (GPEs), and solid polymer electrolytes (SPEs) [12] (Fig. 1).

Despite the encouraging breakthroughs in the field of solid-state polymer electrolytes, considerably, it still has to be accomplished to eliminate the three significant challenges standing in the way of large-scale commercial use of such a stable solid-state electrolyte. Optimizing it is (a) physical and thermal stability, (b) lithium-ion conductivity, and (c) electrode-electrolyte interfacial interaction which is the most important and demanding properties. A polymer-based electrolyte finds it more challenging to get more excellent ionic conductivity beyond 25°C to 30°C, which is considered just

---

✉ S. P. Vijayachamundeeswari
spvijaya.vit63@gmail.com

[1] Department of Physics, School of Advanced Sciences, Vellore Institute of Technology, Vellore 632014, India

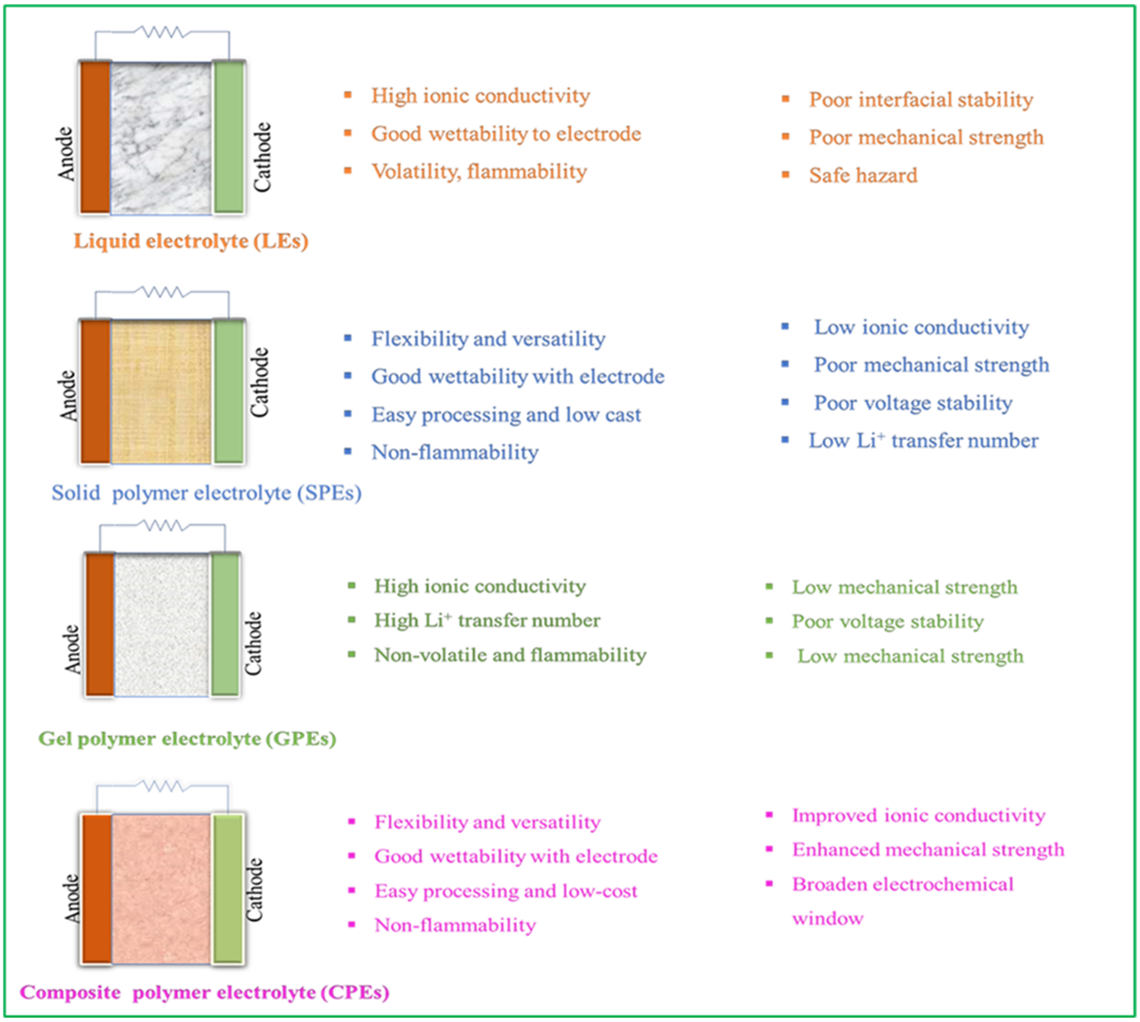

Fig. 1 The properties of liquid and different kinds of polymer electrolytes

under the processing temperature of the battery. However, while operating at high temperatures, polymer-based batteries' thermal stability, mechanical properties, and charging/discharging cycle stability suffer [2, 3, 12–15]. A few strategies are employed to optimize the polymer electrolyte system; notably, interpenetration, cross-linking blending, and co-polymerization are frequently used to coordinate polymer with several other polymers, but they would not considerably improve the electrolyte's mechanical properties. Ionic liquid, fast-ion conductive ceramics, lithium salts, and inert ceramic fillers were among the composites incorporated into the polymer [16]. Utilizing polymeric materials including poly(methyl methacrylate), poly(styrene), poly(ethylene oxide), poly(acrylonitrile), poly(methyl methacrylate), poly(vinylidene fluoride), (polyvinyl chloride) poly(vinylidene chloride-co-acrylonitrile), and poly(methyl methacrylate-co-acrylonitrile), an excellent polymer electrolyte has been produced in lithium-based rechargeable battery.

Composite polymer electrolyte

CPEs primarily exclusively incorporates polymer matrices and Li salts (LiF, $LiNO_3$, LiTFSI, and $LiPF_6$) together with ceramic fillers. It is possible to categorize further the fillers used into active (LLTO, LLZTO, LATP, LGP, etc.) and inactive fillers (TiO_2, SiO_2, Al_2O_3, CeO_2, ZrO_2, SnO_2... etc.) (Fig. 2) [5]. The CPEs' effectiveness can be affected by the essential properties, size, shape, and content of these fillers. The composition of the fillers, in particular, has an essential effect on the efficiency of the CPEs and ion transfer paths. Li-ions are primarily transported by way of the matrix of polymer phases in the composite polymer electrolyte with a small filler content, the permeating network created by the structure of the matrix phase, and the particles of filler in the CPEs with average filler content, and the ongoing ceramic particle phases in the CPEs with elevated filler content [17–20]. Composite electrolytes containing

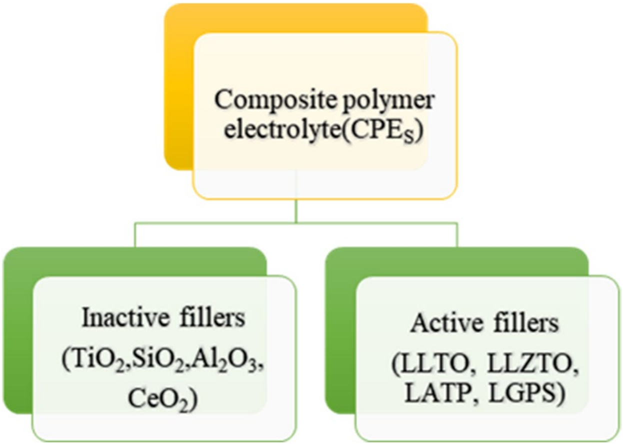

Fig. 2 The classification of composite polymer electrolyte

discrete ceramic fillers communicate substantially reduced ionic conductivity compared to disinfected polymer electrolytes at higher ceramic loadings (>30 vol%). A recent study discovered an elevated interface, a barrier for ion transport across the polymer-ceramic interaction [21]. High temperatures are capable of speeding the breaking down of polymer electrolytes. The chains of polymers could break down at extreme temperatures, leading to decreasing mechanical durability and enhanced ionic conductivity. Thermodynamics can be challenging in applications demanding high-temperature stability, such as fuel cells or batteries. Polymer electrolytes' ionic conductivity can be decreased at low temperatures. The movement of ions throughout the polymer matrix minimizes as temperature decreases, resulting in lowered ion transport, which may impact how they work with devices used in temperatures below freezing [22, 23].

High humidity levels could trigger the polymer electrolyte to take in water. This might prove advantageous for applications where water needs to be present for proton transport, such as proton-exchange membrane fuel cells. Excessive humidity could result in the plasticization or expansion of the polymer, weakening its mechanical integrity and possibly lowering its performance. Low humidity levels could have the opposite direction effect, causing the polymer electrolyte to dehydrate. This may contribute to decreased ionic conductivity because the required water content for ion transport is not maintained. The mechanical characteristics of polymer electrolytes can be altered through high pressure. It could result in changes in the crystallinity or amorphous structure of the polymer, impacting its mechanical properties and performance in general [24–27].

Why polymer electrolyte is required with active fillers

SPEs are in high demand due to the promise of higher energy density, safety, and flexibility with next-generation lithium-ion batteries (LIBs). The major setback of SPEs is their low ionic conductivities, generally ranging from 10^{-8} to 10^{-7} Scm^{-1} at ambient temperature, and exhibit good mechanical characteristics [5]. The excellent conductivity of ions for (GPEs) gel polymer electrolytes at ambient temperature is a benefit (10^{-4} to 10^{-3} Scm^{-1}). This is comparable to the manufacturing electrolyte. Unfortunately, the trouble concerning membranes is that they generally exhibit poor mechanical characteristics since liquid electrolyte absorption has relaxed their physical structure. It plays a vital role in efficient implementations since it can cause problems with winding tension and internal short circuits during cell development and operation [28–30].

Researchers have observed that the involvement of fillers minimizes the polymer's tendency to crystallize or makes a vital impact pathway for ion transport at the interaction among fillers and polymeric, improving the solid polymer electrolyte's ionic conductivity. TiO_2, SiO_2, and Al_2O_3 are inert ceramic fillers that do not contribute to Li-ion conduction [4, 31]. To compare inactive organic filler polymer electrolytes, active inorganic filler-based polymer electrolytes are among the most widely deployed solid electrolytes throughout all batteries. Active filler–based solid polymer electrolytes, including like as perovskite (LLTO) $Li_{0.33}La_{0.557}TiO_3$, garnet (LLZO) $Li_7La_3Zr_2O_{12}$, NASICON (LATP) $Li_{1.3}Al_{0.3}Ti_{1.7}(PO_4)_3$, and sulfide (LGPS) $Li_{10}GeP_2S_{12}$, have high lithium-ion conductivities (1×10^{-3} S cm^{-1}ambient temperature), good thermal stability (ceramics can withstand temperatures >1000°C), and electrochemical window (>5 V) [3, 32]. The addition of active fillers to the mixture changes the molecular makeup of the polymer phases as well as the interaction state of lithium-ion molecules as they communicate with other molecules, including anions and chains of polymers, which influences the motion of lithium ions all through the polymer phase, and this is usually advantageous. Several variables help contribute to more excellent ion conductivity:

(1) The addition of inorganic filler substances reduces the degree of crystallization and glass transition temperature (Tg) of the polymer phase, increasing amorphous conducive areas and accelerating segmental motion.
(2) The lithium salts are simple to dissociate and release a more significant number of lithium ions owing to the Lewis acid-base influence triggered by inorganic fillers.

The many lingering problems of low-energy activation active filler made ion hopping achievable. Active fillers could disperse a significant quantity of lithium ions, increasing the free lithium ions accessible within the active filler-polymer interaction while supporting more swift ion transport [8, 33, 34].

Effect of active fillers on polymer electrolyte

Active fillers are put forward to the enhanced efficiency of polymer electrolytes, which are used in many electrochemical appliances comprising lithium-ion rechargeable batteries and fuel cells. Fillers like these usually consist of inorganic substances applied to the matrix of polymers to improve the electrolyte's conductivity of ions, mechanical strength, electrochemical stability…etc.

Ionic conductivity

Polymers have been employed for embedding active fillers. Active fillers consistently have increased ion conductivity (over 10^{-4} S cm^{-1}). This may be because of several variables, such as the numerous continuous flaws in low activation energy active fillers that enable relatively easy ion hopping. In addition, active fillers may supply an enormous amount of lithium ions, boosting the concentration of free lithium ions at the active filler-polymer interaction. As a consequence, the overall ionic conductivity increases. Perovskite, garnet…etc., and other active fillers were instances [35].

Li^+ transference number

Researchers subsequently examine an attribute associated with ion conduction on the inside of a polymer matrix. The charge transmits and, consequently, the current of an identified ion were directly represented using the transference number. The lithium-ion transference ratio (Li^+) shows the current transported by cations (Li^+) in the electrolytes. It is more beneficial than the lithium content being a high (Li^+) substance to enhance the kinetics of interactions among electrodes and to reduce the gradient of concentration through the battery, permitting the internal voltage drop from the battery to be decreased and the current at its output to be raised. The Lewis acids (the hydrogen molecules of the acid ceramics surfaces) determine a hydrogen connection between the lithium salt anions and the ether's oxygen atoms (Lewis' base). This improves the dissociation of salt and minimizes crystallinity. Consequently, the transference number Li^+ developed, whereas the number of sites containing Lewis' acids decreased, resulting in a higher boost in Li^+ [36].

Mechanical strength

Compared to the polymer matrix, inorganic fillers' insertion enhances tensile strength despite reducing elongation-at-break. Employing a polymer with exceptional viscoelasticity, self-healing, and film-forming capability may result in an active filler's electrolyte with high mechanical stability. The quantity of inorganic fillers present additionally impacts the mechanical properties of electrolytes. Ceramic-in-polymer electrolytes are becoming very adaptable [37].

Electrochemical window

The electrochemical window (ESW) is the voltage that is the difference that exists between the electrolyte's reduction and oxidation potential or the difference of energy between the lowest unoccupied molecular orbital (LUMO) and the highest occupied molecular orbital (HOMO). An ESW is essential for assessing the battery's performance because it demonstrates the limit of electrolytes' resistance to oxidation and reduction [38]. The antioxidant potential of composite polymer electrolytes could be boosted by applying active fillers. This becomes most apparent in how it impacts the polymer's electron-hopping energy levels. On the other hand, grafting optimizes inorganic fillers having polar groups (–OH, –COOH, etc.), which can also help strengthen polymer matrices. On the other side, inorganic filler elemental doping causes imperfections in the surface. These inadequacies can stabilize the lithium salt while optimizing the electrochemical attributes of the electrolyte [35].

Thermal stability

Several processes have been studied and explored to enhance their thermal stability, including cross-linking, creating block copolymers, adding plasticizers, and inserting ceramic fillers. The distribution of ceramic filler materials in a matrix of polymers (relationship between the polymers and ceramics fillers) for the production of CPEs has captured the attention of researchers in the vast majority of these efforts because it has the possibility of helping boost the thermal durability of polymeric electrolytes [39].

Chemical stability

The chemical property of the active filler electrolyte determines storage and manufacturing facilities' situations, and it also impacts the selection of suitable electrode materials. Polymer electrolytes typically exhibit robust chemical stability in the air; however, they must be maintained in an environment with little moisture to prevent H_2O adsorption. Fillers made of inorganic materials can collect contaminants of H_2O or solvents at filler surfaces, preventing H_2O or solvent interaction with the Li anode. It is essential to point out that a polymeric element of the active filler's electrolyte may function as a layer of buffering to prevent direct contact and severe sensitivity of inorganic electrolyte (including Ti-containing oxides, which are LATP and LLTO) with the Li-metal anode [37].

Mechanisms of ion conduction for polymer electrolytes

The ion transfer mechanism is the essential characteristic of ionic conductivity. The motion of vacant positions or interstitial ions in the phase change of bulk composite polymer electrolytes results in fast ion conduction. In contrast, the movement of ions in a matrix of polymers according to an electric field is related to the breaks/formations of bonds of coordination throughout the local segment's motions of chains of polymers, which mostly happens in the amorphous sections. Most solid polymer electrolytes have a maximum ionic conductivity below 10^{-3} S cm^{-1} at ambient temperature [40–42] (Fig. 3).

The amount of moving Li^+ is impacted by the rate of dissolution and dissociation in the lithium salts. The polymers' molecules should work jointly with Li^+ to increase the dissolution degrees within the lithium salts, corresponding to the Lewis acid-base properties. As a result, polar chemicals such as –O–, C=O, –N–, –S–, and C=N are routinely integrated into polymer matrix architectures.

CPEs have an ionic conductivity given by

$$\sigma = \sum n\, q\, \mu$$

Here, n is the number of carriers, q is the ionic charge, and μ is the carrier mobility [43, 44].

The requirement, as mentioned earlier, could potentially be encountered by commonly employed active fillers such as LLTO (perovskite), LLZO (garnet), LAGP (NASICON), and LGPS (sulfide), and the ion conductivity of the majority of composite polymer electrolytes is well achieved 10^{-3} S cm^{-1} at ambient temperature. Active filler reinforcing the mentioned ion-conducting routes occurs in composite polymer electrolytes, and incredible beneficial effects are accomplished. This ceramic layer acts as a plasticizer, diminishing polymer crystallinity and increasing the proportion of amorphous structure, enhancing lithium-ion mobility. Additionally, the acidic compounds on the surface of ceramics possess a powerful attraction for anions, facilitating the dissociation of lithium salts, which gives rise to a more significant amount of free Li-ion. Similarly, numerous vacant spaces occur on the surfaces of ceramics, enabling lithium ions to hop among the two and consequently offering a more manageable way compared to polymeric electrolytes [20, 45–47]. Some ion transmission models have been mentioned, notably Vogel-Tamman-Fulcher (VTF), Arrhenius, Williams–Landel–Ferry (WLF), and free-volume models (Fig. 4).

Vogel-Tamman-Fulcher

The VTF equation is also fulfilled by the polymeric segments' mobility and the conductivity of the ion relationship.

$$\sigma = AT^{0.5\ \mathrm{e}^{-\mathrm{Ea}/k(T-T_0)}}$$

A is the pre-exponential factor, Ea is the apparent activation energy, K is a constant, T is the ambient temperature, and T_0 is the ideal glass transition temperature. It is generally considered that Tg is 50 K lower than the glass transition temperature (Tg) [48].

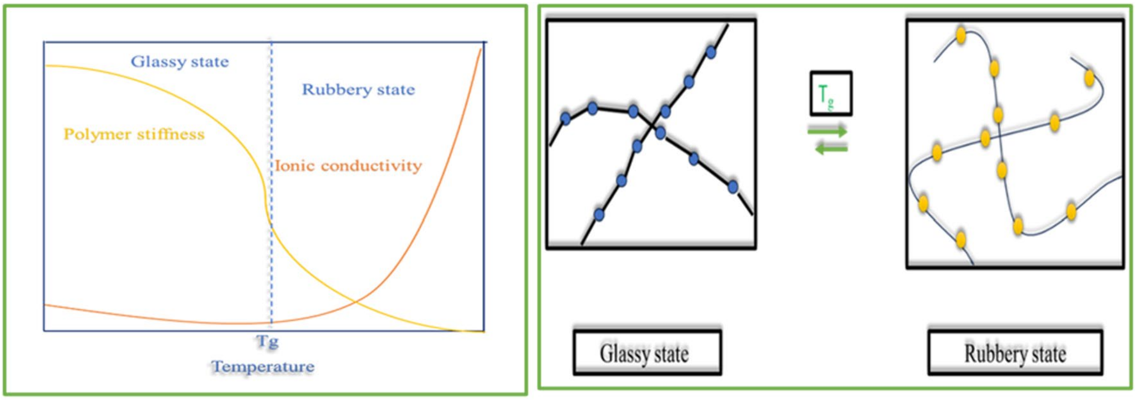

(A) (B)

Fig. 3 **A** The relationship between polymer stiffness and ionic conductivity, and (**B**) the behavior of polymer segments above and below the glass transition temperature, which promotes ion conduction

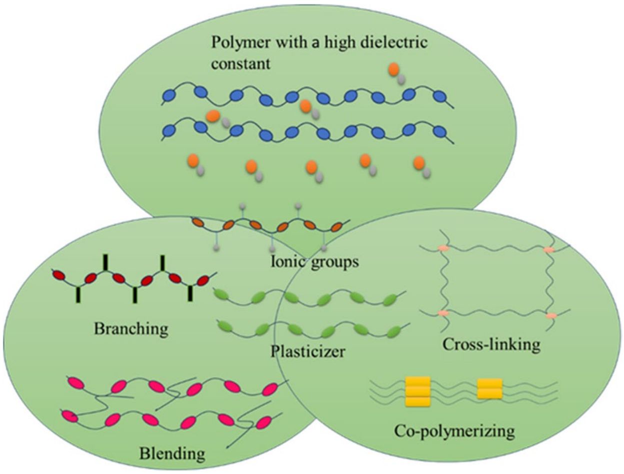

Fig. 4 The strategies for improving the ion conductivity of polymer electrolytes

The VTF equation indicates that Li^+ transportation is linked to the polymer chain segmentation movement. Li^+ transfer in SPEs frequently happens mainly in the amorphous space above Tg. Polymers with a lower Tg exhibit greater segment mobility, which at first may promote the movement of ions and consequently boost the conductivity of ions. The VTF model additionally indicates that minimizing activation energy may increase ionic conductivity; consequently, eliminating a high amount of lithium salts has advantages for swift ion transport [49].

Arrhenius model

As shown here, the equation developed by Arrhenius may be utilized to describe ion hopping.

$$\sigma = A/T\mathrm{e}^{-\mathrm{Ea}/RT}$$

where σ is the ionic conductivity, *A* is the pre-exponential factor, *T* is the ambient temperature, Ea is the apparent activation energy, and *R* is the ideal constant.

The Arrhenius model formula demonstrates that raising the temperature and decreasing the activation energy can significantly improve the conductivity of ionic compounds. The polymer's backbone and accessory chains' movement frequency and amplitude should similarly increase. The coordination grows more precise as temperatures rise. The amorphous polymer's segmental motion would become fully dissociated from the movement of the ions, and ions would have to use less energy to jump from one location to another [50, 51].

Free volume model

The vibration within chain molecules in polymeric electrolytes may influence the space around the molecular chains, resulting in vacancies and accessible spaces. The free volume of polymer electrolytes can be influenced by the molecular weight of their end groups, the temperature, and the lithium salt. The free volume model concept highlights that the free volume dimension determines the migration of ions and electrolytes' conductivity of ions. Somebody has connected the free volume to polymer segment motion and discovered that boosted free volume might enhance polymer segment motion.

The inverse proportion of the free volume fraction can be roughly linearly connected to the logarithmic of ionic conductivity.

$$\mathrm{In}\ \sigma = \sigma^{*} + \beta/\mathrm{f}_{\mathrm{V}}$$

where fv is the free volume fraction, σ* is the ionic conductivity at the highest free volume fraction, and β is the activation coefficient of the thermal free volume fraction.

As mentioned before, the free volume model formula above demonstrates that temperature enormously affects free volume. While temperatures grow, the polymeric segment's vibrating ability improves to overcome potential barriers to movement between locations, and the process of expansion produces additional free volume that encourages the transportation of the polymeric sections, Li^+, or solved molecule. Consequently, a boost in the conductivity of ions may additionally be related to enhancements in polymer segmentation movement and ions' hopping capability [52].

Williams–Landel–Ferry model

The Williams-Landel-Ferry equation has been developed after improving the VTF equation to account for the consequences of polymer viscosity and chain segment relaxation.

$$\mathrm{Log\ aT} = \left\{\left(-\mathrm{C}_1\right)\left(\mathrm{T}-\mathrm{T}_{\mathrm{S}}\right)/\left(\mathrm{C}_2\right) + (\mathrm{T}-\mathrm{Ts})\right\}$$

where aT is the displacement factor, which represents the ratio of the relaxation time of the chain segments, and Ts is the reference temperature, usually represented by Tg. C_1 and C_2 are constants [30, 37].

The WLF formula additionally demonstrates, therefore, that the volume of freedom has influenced the movement of ions in polymer electrolytes and that the micro-Brownian movement of chain segments has an essential effect on ion transport in amorphous domains. Decreased Tg is one more advantageous approach to improving the mobility of polymer segments with excellent ionic conductivity. Ions that are charged could readily travel in the space provided by the polymer-free volume and migrate among sites of coordination along chains of polymers exceeding the Tg. The WLF designs also prioritize the significance of free volume and the surrounding temperature, and expanding the temperature may substantially alter the free volume size/fraction and crystallization; nevertheless, enhancing the operating temperature of solid-state lithium-ion batteries for fast ion transmission would not be practical [53, 54].

The interface between the electrode and electrolyte

The interface between the electrodes and the electrolyte plays a role in how a battery performs. This becomes more crucial when using composite polymer electrolytes. To achieve performance in lithium-based batteries, it is essential to establish an efficient interface between the composite polymer electrolyte and the electrodes [55].

However, it is worth noting that even though most composite polymer electrolytes handle the movement of lithium ions, we should recognize the conduction of ions at the point where the electrode and electrolyte meet. This ion conduction at the electrode interface differs from during most phases in composite polymer electrolytes. Additionally, establishing a connection between the electrolyte and electrode remains challenging for solid-state lithium batteries (SSLBs). Various factors, like how the electrolyte and electrode interact, as growth and disintegration in high-pressure areas, all impact interface stability. When it comes to the batteries made with CPEs, three types of interfaces are involved: the connection between the anode and CPEs, the interface between the cathode and CPEs, and finally, the interface between fillers and polymer materials [56–58]. In the years, there has been increasing attention given to composite polymer electrolytes consisting of both organic and inorganic components as a solution to tackle these problems (Fig. 5).

Developments of the CPEs/cathode interfaces

The electrolytes generate numerous polarization regions because of interactions between molecules in an electrical field, decreasing electromechanical features [59]. High-voltage compatibility of the electrolyte indicates its ability to withstand oxidative breakdown thermodynamically. Every component of the electrolytes (polymers, lithium salts, additives, etc.) needs to possess a lower maximum occupied molecular orbital (HOMO) compared to the cathode. Utilizing Lewis acid and base correlations (vacancy, dipole-to-dipole correlations, and hydrogen bonding) with polymeric and lithium salts, inorganic fillers can enhance the electrochemical capacity of CPEs [60].

The cathode/electrolyte interaction necessitates solid electrolytes with excellent adaptability to offer low interaction resistance. As a result of comparing the high viscosity and flexibility of the two-component composite cathode and the electrolyte, no holes or voids were found in the interface regions, enabling the cathode's close interaction with the CPEs and minimal interface impedance [61]. The transport of the ions and electrons inside a cathode is equally essential as the cathode/electrolyte interaction in pursuing the high energy density and expanded life span of the all-solid-state batteries. Establishing ion/electron conducting routes in both the cathode and interfaces is vital for reducing polarization while maintaining the battery's total capacity [34, 62, 63].

Furthermore, compared to beneficial interaction and an established incorporated conducting network, the broad electrochemical window of CPEs needs to be present for developing a stable connection between cathode and CPEs, which is crucial for applying high-voltage cathode in high-energy-density systems [64, 65]. Overall, the electrochemical range of polymer electrolytes is less than 5 volts vs. Li/

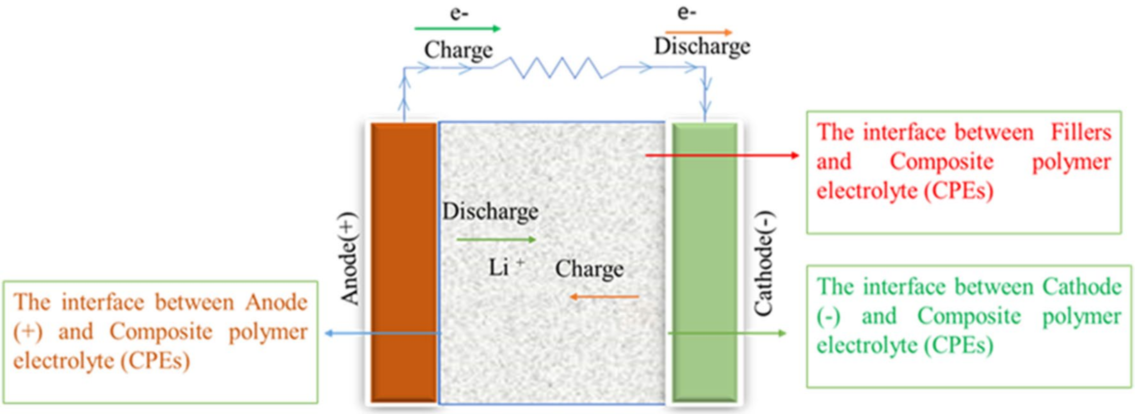

Fig. 5 The interface between electrode and electrolyte

Li$^+$; nevertheless, ceramics electrolytes can reach up to 9V or even higher. For CPEs, a ceramic filler could increase the electrochemical window above 5V, allowing most cathode materials with substantial operating voltage voltages to be supported. Generally, a higher ceramic concentration may enhance electrochemical stability [66, 67].

Developments of the CPEs/anode interfaces

On the contrary, the anode/electrolyte connection needed a solid electrolyte to survive through the penetration of metal lithium dendrites. The minimal interface resistance can be achieved due to the flexibility of the polymer electrolytes, regardless of the low mechanical characteristics that make it impossible for them to endure the absorption of the metallic lithium dendrite [68, 69]. The polymer host offers continuous ion-conducting networks and safeguards ceramic fragments from the electrode to minimize adverse effects; nonetheless, they also offer kind interaction with electrodes for reducing Li-ion transfer resistance, possibly establishing a uniform Li-ion movement and preventing lithium dendrite creation. Owing to the insufficient connection that exists between the lithium anode and the CPEs, too much impedance and heterogeneous lithium-ion deposition happen, leading to unsatisfactory rate stability and uncontrollable lithium dendrite growth possess excellent compatibility with Li metal and functions effectively in suppressing lithium dendrite development [70, 71].

Lithium dendrites have the potential to penetrate the electrolyte, establishing contact with both the cathodes and anodes. Recent research suggests incorporating inorganic additives can enhance the compatibility between the solid-state electrolyte and the anode [72–74]. These are some of the roles played by additives in reducing interfacial issues. Firstly, they help regulate ions' movement in the electrolyte's bulk phase, ensuring a more uniform distribution of lithium ions [75]. This regulation helps control and prevent the formation of lithium dendrites at their source. Secondly, these additives increase the strength of CPEs, which helps suppress lithium formation and dendrite growth [76, 77].

Interface between fillers and polymer materials

The interface challenges can develop among electrodes and CPEs and chains of polymers and ceramic fillers. Numerous investigations have already been performed to identify novel techniques for improving the interface between polymers and ceramics. Despite the interactions connecting ceramic nanoparticles and polymer chains in CPEs attracting fewer resources, it is of the utmost importance to supply a low-resistance connection between ceramic and polymer for outstanding performance in all-solid-state batteries [78]. To enhance the performance of all solid-state rechargeable batteries, it is possible that improving the interactions between fillers and polymer chains in CPEs could effectively address the underlying issues associated with CPEs [79]. The uniformly distributed dispersion of ceramic fillers certainly contributes to constructing continuous fast speeds and equal Li-ion migration channels because of the high ions conducting the interphase between ceramics and polymer. Ceramics particle dimension, form, structure, and three-dimensional ceramic framework in CPEs affect the interface characteristics between ceramic and polymer. Considering that interface investigation is at the beginning stages, multiple states of different chemical and physical addresses have been employed for creating an optimal ceramic-polymer interface, which is crucial for promoting the creation and application of all-solid-state lithium battery packs [80].

Influence of size, dimensionality, concentration, and alignment of filler in polymer electrolyte

Size

The overall size of particles of engraved materials like ceramics significantly impacts the conductivity of ions of SPEs. Particles that are smaller that have a greater specific area of surface and a more significant number of abundant active sites could make the host more crystalline of polymer substrates and help promote the disintegrating of the lithium salts with greater efficiency, generating numerous ion-conducting pathways transporting lithium charges. The formation of long-range lithium-ion channels with long ranges with consequently powerful ionic conductivity is made possible by the nano- and micro-meter scales. Nano-sized particles also accelerate the advancement of polymer electrolyte ion conductivity, and their more minor size results in higher ionic conductivity. Due to their high surface energy, ceramic material nanoparticles rely primarily on aggregating and separating phases in a polymer matrix, to guarantee high polymer electrolyte standardization and prevent nonuniform lithium-ion (Li$^+$) transport [10, 80, 81].

Dimensionality

The ceramic electrolyte's shape directly influences the path and dimension associated with the lithium-ion direction; they are the amount of supply. Nanomaterials have also been divided as zero-dimensional (0D) (which includes nanoparticles), one-dimensional (1D) (including variables such as nanotubes and nanorods), two-dimensional (2D) (such as graphene), and three-dimensional (3D) as well (such as nano prisms and nanoflowers). By reducing polymer crystallinity while providing more extraordinary Li^+ diffusion pathways to CPEs, (0D) nanoparticles could enhance Li^+ conductivity and mechanical strength. Despite significantly improving Li^+ conductivity, soft CPEs with low percolating threshold values (30 wt%) cannot successfully prevent lithium dendrite development [78]. For CPEs, an interconnecting framework has been constructed for elaborately generated 2D LLZO nanosheets or 3D LLZO nanowires. Furthermore, it provides broadened ionic conduction of the channels [82] (Fig 6).

Nevertheless, substantial agglomerate associated with this filler may persist, decreasing the composite electrolytes' long-term effectiveness. A middle layer between stiff inorganic fillers and an organic polymer matrix must be constructed to tackle this interface compatibility problem and permit a consistent distribution of inorganic additives with high content [24]. The enhanced performance in the conductivity of ions could be attributed essentially to the achievement of a continuously 3D ion-conducting networking path that offers far-reaching rapid lithium-ion transmission pathways. As an outcome, especially in comparison with ceramics nanoparticles, the nanowires, fibers, and nanosheets in the polymer substrate can provide continuous Li-ion transportation pathways, contributing to the more effective conductivity of ions. In addition, ceramics fillers' nanowires, fiber, and nanosheets could be used for the construction of 3D or 2D lithium-ion transport routes and networks for high-efficiency, far-reaching lithium-ion transmission [20, 80].

Alignment of filler

Inorganic substances in polymers enable one to utilize CPEs completely. Inorganic compounds are frequently spread randomly in polymers. The included number of inorganic fillers causes disruptions in polymer crystallization, increasing the conductivity of CPE ions. Nevertheless, filler substances will inevitably come into the polymer, prohibiting the formation of a percolating network. Subsequently, it is feasible to generate percolating networks by promoting the dispersion and transport of fillers in polymers. The inorganic fillers and polymers interact via Lewis' acid-base interaction. The idea behind it is based on the presumption that fast-ion-conducting pathways could have been constructed on the surface of the filler. Ceramic filler materials have developed from solitary 0D particles, 1D nanowires, and 2D nanosheets to continuous three-dimensional frameworks and bulk components. There are (0D and 1D) inorganic fillers randomly distributed throughout the polymer chains, whose distribution is similarly irregularly disseminated. Li-ions that pass through channels in solid composite electrolytes appear disorganized since nanoparticles and nanowires are distributed randomly within the polymer matrix. Considering various ceramics with different structures, nanowires significantly boost the conductivity of ions in polymeric electrolytes [82].

Additionally, due to their structural characteristics, 2D fillers have immense significance. Small-sized,

Fig. 6 The dimensionality. **A** Nanoparticles, **B** nanorod, **C** nanoplates, **D** nanofiber

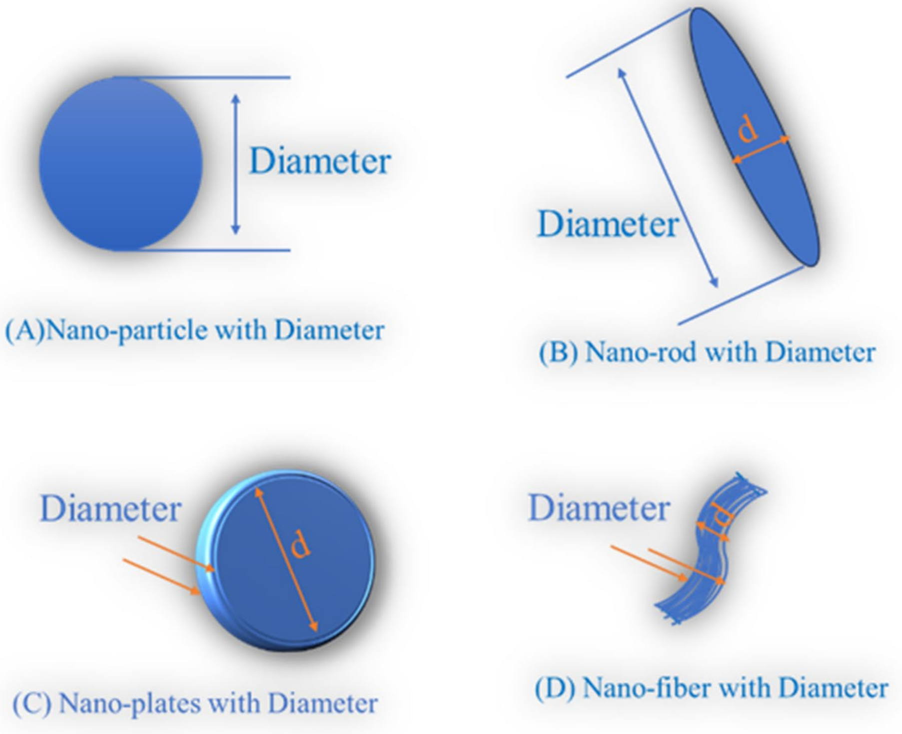

two-dimensional nanosheets are becoming increasingly common among researchers for practical applications. This is caused by the challenge of offering continuous transport of ion pathways in the large dimensions of 2D nanosheets of material. In addition, larger-size 2-dimensional nanosheets show very little ability to prevent polymeric matrix crystallization. Nevertheless, 2-dimensional fillers possess a high specific surface area, a fragile spherical structure, and a substantial aspect ratio. Whenever the size of the 2D nanosheet is small enough, a more significant contact area between it and the polymer matrix could be produced. Among the 2D nanosheet-polymer interactions, additional ion conductivity will be constructed, culminating in improved ionic conductivity. In the polymer matrix, the additive (3D) swiftly aggregates. A successful approach for addressing the dispersion mentioned above is to build a 3D framework by controlling the position of the filler space in the polymers. Moreover, the inorganic system has excellent mechanical strength, enabling it to prevent lithium dendrites from forming while boosting cycle stability [20, 83] (Fig. 7).

Concentration of fillers

The filler concentration polymer electrolytes have vital functions. The functional structures on the surface of inorganic additives will additionally impact carrier concentration in composite polymer electrolytes and polymer chain movement. The intrinsic transport of ions reflects these variances in effectiveness. Furthermore, some filler quantities can improve the relationship between the electrode and the electrolyte by acting synergistically and lowering the ion transport barrier at the interface. Additionally, because of the many continuous inefficiencies in active fillers that have low energy of activation that enables facile ion hopping, active fillers may provide an enormous amount of lithium ions, thereby increasing the number of free ions of lithium at the point of contact between the active filler and the polymer itself [78]. As a consequence, the general conductivity of ions changes. perovskite, garnet, LISICON, and various other active fillers are examples. Whenever the active filler ratio is below 40%, CPEs could provide a significant amount of free lithium ions. Once the concentration of active filler exceeds a specific point, it forms a porous network. The way ions behave in transportation mechanisms is shifting at the moment. The specific quantity concentration of inorganic additives and polymers includes the complex relationship of the Lewis acid-base connection. This is based on the presumption that fast-ion-conducting communication could have been developed on the surface of the filler conductivity of ions of frequently employed active fillers for polymers. Active fillers were familiar with excellent ion conductivity (> 10^{-4} S cm^{-1}) [20].

Properties of lithium salt

In the case of lithium batteries, the electrolytes act like an interface over ion transfer between negative and positive electrodes. Lithium salt is the supplier of the lithium-ions in the polymeric electrolyte (not the single-ion polymer electrolyte), has become a vital component of the electrolyte, and has a significant impact on the battery's functionality variables, including capability, beneficial temperatures, cycle capability, and security accomplishments. The nature and quantity of lithium salts present have an essential effect not merely on the polymer's solid-state electrolyte's film-forming capacity but additionally on the conductivity of ions

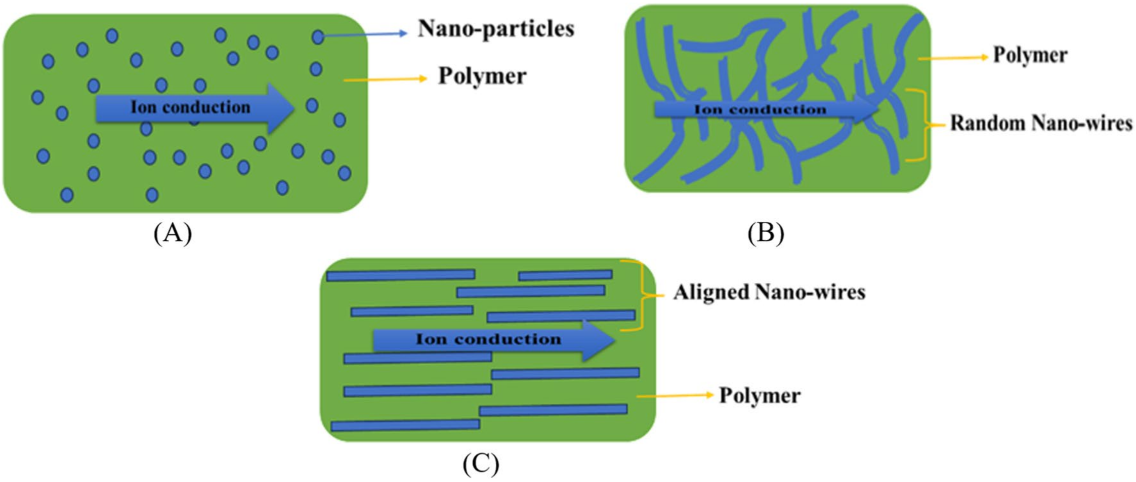

Fig. 7 The (**A**) alignment of nanoparticles (NPs), **B** alignment of random nanowires (NWs), **C** aligned nanowires (NWs) conducting channels involving the lithium ions transport in composite polymer electrolytes

and interfacial durability of the electrolyte's solid state and the electrodes themselves (Table 1)

Relationships of polymer, lithium salt, and inorganic fillers

The polymers, inorganic filler, and lithium salt simultaneously interplay in composite polymer electrolyte. This relationship is accomplished mainly through two distinct forms:

- The connection that occurs exists between the filler and the lithium salt. This is accomplished by altering the chemical environment of lithium-ion batteries.
- The relationship between the filler and the polymer is primarily seen in shifts in the conductivity of ions and Li^+. Modifications in the polymer aggregated architecture have been involved. It is identified by the degree of crystallinity, glass transition temperature, and spherulites [35].

Interacting between polymers and inorganic fillers

Since the inorganic fillers can frequently be very tiny sized and equally spread within the polymer matrix, there are additionally numerous insignificant interfacial fields in the whole composites' polymer electrolyte. Adding to that, maintaining the condition of these interface locations is difficult due to the substantial differences in chemical and physical properties between the matrix of polymers and inorganic ceramics fillers. Surfaces of inorganic filling agents are defect-rich and highly receptive, helping particles to come into contact with different elements and create complicated interface regions. For example, composite electrolytes established from active organic fillers and a polymer substrate are one option. Compared to the mixture of the polymer matrix and lithium salts, active fillers are lithium-rich, and the state of lithium ions in the interfacial regions changes substantially from those that qualify the vast majority of the polymer matrix and active fillers. These modifications significantly alter the lithium-ion conducting pathways [33].

Interacting between polymers and lithium salts

The fundamental ion-dipole relationship among ions and polymers is the reason for the lithium salt disassociation. It is the essential factor responsible for liberated concentrations of ions and having a significant impact on ionic conductivity. In addition, the relationship between anion and anion receiver could boost the lithium ion's transfer number, thus decreasing the polarization of concentration of lithium batteries. As a result of its strong polarity, plastic crystals might reduce the chemical interaction capability of Li^+ by polymers and ionize lithium salt, which makes it favorable to the decomplexation of Li^+ by polymers, which contributes to a boost in the conductivity of ions. The ion-dipole relationship possesses an essential impact on ionic conductivity likewise. The ionic conductivity was highest among polyethers at a salt level of 5 mol%. The conductivity was reduced, and the Tg value gradually enhanced with increasing lithium-salt concentrations to 5 mol%. Owing to the significant attraction among polyether and Li^+, cross-linking formations have been formed, limiting segmental movements within local chains [91].

Interacting between fillers and lithium salt

The groups of chemicals occur upon the surfaces of inorganic fillers. A combination of the lithium salts, such fillers exhibit significant Lewis acid-base interaction. Bonds of hydrogen, holes, and dipole-dipole relationships are characteristics of this interaction [92]. The effective reactions between lithium salt anionic groups and ceramics filler groups of chemicals promote lithium salt dissociation and boost free Li^+ concentration at the point of interaction [93]. The unique properties of chemicals on the outer surface of inorganic additives may interact with lithium ions to weaken the bonds between lithium-ion and polymer compounds, allowing lithium ions to travel considerably faster [52].

Type of active fillers

Active fillers are essential additions to composite polymer electrolytes. They have several benefits, notably increased thermal stability, mechanical strength, and electrochemical performance. By thoughtfully choosing and introducing suitable active fillers, investigators could modify the characteristics of CPEs according to the specific demands of different electromechanical electronic gadgets, offering the possibility of intriguing and efficient energy preservation and conversion technologies. Crucial additions. They have several benefits, notably increased electrochemical performance, thermal stability, and mechanical strength (Fig. 8).

Garnet-type composite polymer electrolytes

The most recent identification of (LLZO) garnet-type material electrolytes has been viewed as one of those most appealing along with essential electrolytes for solid-state batteries, with potential advantages in substantial electrochemical stability (>6 V versus Li/Li^+ from CV experiments), excellent thermal strength, energy density, safety, and high ionic conductivity (range 10^{-4} to 10^{-3} S/cm), which offer an outstanding possibility for battery technology [90]. The crystal structure-based garnet-type filler (LLZO)

Table 1 The properties of lithium salt

Lithium salt	Diagram	Properties	Ref.
Lithium perchlorate ($LiClO_4$)	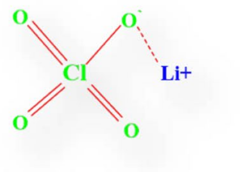	➢ High solubility ➢ High ionic conductivity ➢ High oxidation ability ➢ Low cost	[84]
Lithium hexafluorophosphate ($LiPF_6$)	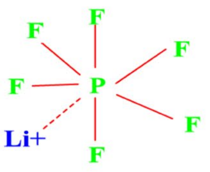	➢ High solubility ➢ form SEI film ➢ Low stability	[85-86]
Lithium hexafluoro arsenate ($LiAsF_6$)	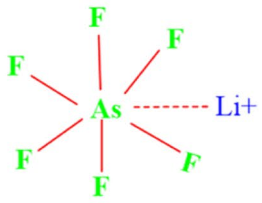	➢ High chemical stability ➢ No current collector corrosivity ➢ As the element is poisonous	[56]
Lithium bis (trifluoro methane sulfonyl) imide (LiTFSI)	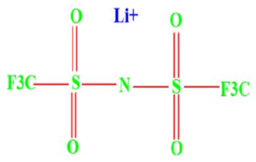	➢ The high ionic conductivity, ➢ High thermal stability, ➢ Corrosive to current collectors	[87]
Lithium bis(oxalate)borate (LiBOB)	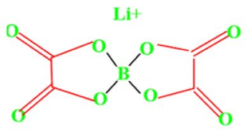	➢ High ionic conductivity ➢ Passivation of electrodes ➢ Low solubility	[88]
Lithium tetrafluoroborate ($LiBF_4$)	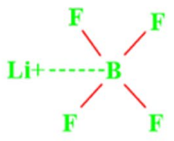	➢ Suitable for both high and low temperatures ➢ Low ionic conductivity ➢ High thermal stability	[89]
Lithium difluoro(ethanedioato)borate (LiODFB)	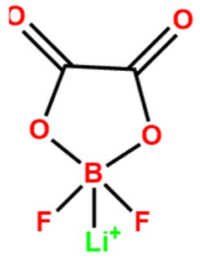	➢ From SEI film ➢ No current collector corrosivity ➢ Good low-temperature performance ➢ High cost	[90]

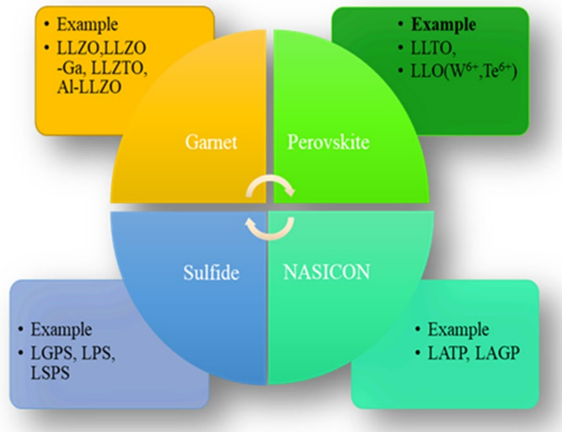

Fig. 8 The types of active fillers

classified into two types: the first one is cubic (space group Ia-3d, cubic-LLZO) and the second is tetragonal (space group I41-acd, tetragonal-LLZO) crystal structures. The fundamental disadvantage of the tetragonal LLZO is its poor lithium-ion conductivity of 10^{-6} S cm^{-1}, whereas the cubic LLZO has a desirable high ionic conductivity of 10^{-4} S cm^{-1}. However, at room temperature, a cubic crystal shape is unsustainable [94].

To improve the room temperature stability of cubic LLZO, doped super-valent cations include Al^{3+} and Ga^{3+}. Additionally, multiple elements like Nb^{5+} and Ti^{4+} have been incorporated into the cubic LLZO crystalline structure to enhance its conductivity massively. The above component-doped LLZO displays conductivity ions of up to 10^{-3} S/cm at average temperature and remarkable chemical strength across a broad range of temperatures [95–97]. In addition to the conceptual design, one of the most notable improvements in garnet-type solid electrolytes should generate future electrolyte growth. At ambient temperature, Ta-doped LLZO ceramics electrolyte (LLZTO) does have a Li^+ ion conductivity of 10^{-4} to 10^{-3} Scm^{-1}, which would be considerably greater than LLZO and even comparable to conventional aqueous electrolytes. Ta-doped LLZTO-polymer composite electrolytes have also been researched by incorporating Ta-doped LLZTO particles into the polymeric matrix, which have characteristics including lightweight, good processability, and good electrode contact. Unfortunately, overall, Li^+ transfer numbers are slightly lower than 0.8 owing to the inert matrix of polymer, and heating treatment above 150 °C continues to be needed to dissolve the polymers and produce composite electrolytes [89]. Ting Yang et al. demonstrate that by adding just 5% to a ceramics filler that includes untreated cubic-phase LLZO nanowires, as Al-doped and Ta-doped LLZO nanowires, composite polymer electrolytes ionic conductivities in the 10^{-4} S/cm range at 20°C [98]. To stabilize the cubic LLZO and generate Li-ion vacancy, super-valent cation substitution on the Zr sites (16b) was affected. Ta-enriched LLZO with only a factor of 0.5, $Li_{6.5}La_3Zr_{1.5}Ta_{0.5}O_{12}$ (LLTZO), offers the greatest vacancy allowing Li-ion transmission [99].

Yi, Maoyi, et al. show that Ga-doped $Li_7La_3Zr_2O_{12}$ (Ga-LLZO) is a potential solid electrolyte with a more excellent Li-ion conductivity of 5×10^{-3} S/cm at 30°C and an activation energy of 0.28 eV [100]. Dopants are substances that have the potential to enhance the number of vacancies disordered within the Li sub-lattice, accelerate improved hopping pathways for Li^+, and enhance conductivity. The replacement of 0.2–0.24 mol of aluminum (oxidation of Al^{3+}) for lithium (Li) outcomes in a generation of 0.4–0.48 mol of lithium (Li^+) vacancy each LLZO unit of formula and maintains the cubic phases at 298 K, the conductivity of ionic substances increases to 0.4 mS/cm throughout this phase of the reaction, and Ta^{5+} doping has been selected over Al-doped for the reason that Ta. At the same time, Al is not positioned on the Li sublattice, which consequently offers more substantial conductivity. As a matter of fact, at 298K, $Li_{6.5}La_3Zr_{1.5}Ta_{0.5}O_{12}$ (0.5 lithium (Li) vacancy per formula unit) is blessed with a conductivity of ions within the proximity of 1 S/cm [101–103] (Table 2).

NASICON-type composite polymer electrolyte

The solid electrolyte material NASICON-type (LATP) (Na-Super-Ionic Conductor) has been frequently utilized in CPEs for lithium (Li^+)-based batteries because it exhibits a significant increase in conductivity when compared to other substances with equivalent crystal framework [116]. For describing the prospective structures of crystals of NASICON materials, three types of systems are frequently utilized:

1. NASICON: C2/c, ~ a 15.1Å, b~ 8.7Å, c~ 21.6Å, and 90.2°, which generally occurs at temperatures near 300 K.
2. NASICON: C2/c, a 15.1Å, b~ 8.7Å, c~ 8.8Å, and 124°, which occurs at temperatures ranging from 300 to 450 K.
3. NASICON: R3c, an~ 8.7Å, and c 21.9Å, the highest symmetry framework in the NASICON substances, could be accomplished above 450 K.

The broad spectrum of attainable combinations within the fundamental formula is an exciting component of NASICON building construction. $Na_xM_2(SiO_4)_z(PO_4)3z$, whereby x may fluctuate bounded by 0 and 4 M, can be divalent, trivalent, tetravalent, and pentavalent transitional metal cations. By swapping the location of the (M) site, electrochemical and

Table 2 The properties of Garnet-based composite-based polymer electrolytes (GCPEs)

Polymer	Lithium salt	Garnet (wt%)	Ionic conductivity with temperature	Li^+ trans	Electrochemical stability (V)	Mechanical strength (MPa)	Ref
PEO	$LiClO_4$	50 wt% LLZO	1.4×10^{-4} scm^{-1} at RT	–	5.2	–	[99]
PEO	$LiClO_4$	5wt% Al-doped LLZO NWs	1.27×10^{-4} s cm^{-1} at 20°C	–	–	–	[104]
		5wt% Ta-doped LLZO NWs	1.50×10^{-4} s cm^{-1} at 20°C				
		BM-LLZO NPs	1.50×10^{-4} scm^{-1} at 20°C				
PEO	LiTFSI	LLZO	0.89×10^{-4} S cm^{-1} at RT	–	–	–	[101]
PAN	$LiClO_4$	LLZO	1.60×10^{-3} Scm^{-1} at 25°C	–	4.5	–	[105]
PVDF/PEO	LiTFSI	LLZTO	9.30×10^{-4} S cm^{-1} at 50°C	–	–	–	[106]
PEO	LiTFSI	LLZNO	5.23×10^{-5} Scm^{-1} at RT	–	5.2	–	[107]
			1.4×10^{-3} S cm^{-1} at 60°C				
PVDF-HFP	LiTFSI	LLZO	9.5×10^{-4} S cm^{-1} at RT	–	5.2	–	[108]
PEO	$LiClO_4$	LLZA	1.29×10^{-5}S/cm at 25°C	–	4.6	–	[109]
PEO	$LiClO_4$	15wt% LLZNb	3.6×10^{-4} S cm^{-1} at RT	–	–	–	[110]
PEO/(PVDF-HFP)	LiTFSI	LLZTO	3.3×10^{-4} S cm^{-1} at 40°C	0.52	5.0	–	[98]
PEO	LiTFSI	LLZTO	2.1×10^{-4} S cm^{-1} at 30°C	0.46	4.7	–	[111]
			5.6×10^{-4} S cm^{-1} at 60°C				
PEO	$LiClO_4$	LLZO	4.42×10^{-4} S cm^{-1} at 60°C	–	–	–	[112]
PEO	LiTFSI	LLZTO-SN	1.22×10^{-4} S cm^{-1} at 30 °C	0.40	5.5	–	[113]
PEO	$LiClO_4$	LLZTO	4.8×10^{-4} Scm^{-1} at 60°C	0.16	4.6	–	[114]
			1×10^{-4} Scm^{-1} at 80 °C	0.20			
PEO		LLZO-Al	8.5×10^{-5} S cm^{-1} at RT	–	–	–	[115]

ion conduction attributes may be adjusted for specific applications [117]. The NASICON type has two phases. First, the conducting phase is $LiTi_2(PO_4)_3$ (LTP), while the insulating phase is $(AlPO_4)$ (ALP). Its conducting phase $LiTi_2(PO_4)_3$ (LTP) is made up of voids in a 3-D system of conductivity routes, and interstitial Li^+ ions migrate through the conduction routes via ultrafast and slower modes. At the room's temperature, the overall conductivity is 10^{-3}S/cm. On the other hand, LATP's boundary grain conductivity is several orders of magnitude lower than its bulk value, decreasing the total operational effectiveness of a solid-state battery. Ordinary grain boundary conductivity has been caused by a combination of variables, including low density because of grain spacing, the existence of insulating additional phases such as $AlPO_4$ at the grain boundary, and decreased size of particles due to a diminished sintering capability. Secondary phases can be generated in modest quantities by adding the lattice with the trivalent elements Sc^{3+} and Y^{3+}, with an ionic radius more remarkable than the equivalent host cations (Ti^{4+}). The s preparation process causes second-phase separation at the grain boundaries [118, 119]. The conducting phase LTP structural unit is constructed from up of TiO_6 octahedrons and PO_4 tetrahedrons, which form a three-dimensional interconnected channel that is excellent for lithium-ion transfer. In the meantime, a partial substitution of trivalent cations (Al^{3+}, Fe^{3+}, and Y^{3+}, for example) may significantly improve ionic conductivity. Following the investigation, partial replacement of Ti^{4+} in the LTP crystal structure with Al^{3+} ions to generate $Li_{1.3}Al_{0.3}Ti_{1.7}(PO_4)_3$ (LATP) could boost the conductivity of ions through improving concentrations of carriers and system configurations by preventing Ti^{4+} oxidization [120].

The particular gel polymer electrolyte (GPE) membranes exhibit insufficient mechanical strength, especially after electrolyte uptake. $Li_{1.5}Al_{0.5}Ti_{1.5}(PO_4)_3$ (LATP) has been distributed or embedded in the gel polymer matrix to enhance mechanical stability. Furthermore, the connection of inorganic particles using electrolytes made of polymers has been extensively researched [115]. As a consequence of their high lithium-ion conductivity and expansive electrochemical windows, NASICON-type (LATP) composite form substances $Li_{1+x}Al_xM_{2-x}(PO_4)_3$ (M = Zr, Ge, Ti, etc.) have been receiving a lot of interest as solid electrolyte substances, thereby providing a natural match for the electrolyte substance in extremely all-solid-state lithium-ion batteries having a high voltage and glass-ceramics with NASICON-type structured compound (LAGP) which offer better stability as well as elevated relative densities due to a substantially more solid microstructure compared to LAGP ceramics [121]. The NASICON-type structured (LATP) more effectively both air and water stability owing to strong P–O bond correlations within the LATP framework and having low relative density ~2.9 g/cm^3 versus 5.1 g/cm^3 for $Li_7La_3Zr_2O_{12}$ [122].

Several beneficial techniques, which include incorporating the sintering disabilities, enhancing the procedure for sintering, and doping, also known as elements via a solid electrolyte structure, are frequently employed to improve its capacity to transport lithium ions around within solid electrolytes as well as elements' doping systems utilized which is a simple and effective way of improving both the physical and electrochemical characteristics of LATP solid electrolytes. Further investigations on Si^{4+}, Y^{3+}, Ge^{4+}, Ga^{3+}, and Nb^{4+} suggested that doped and inclusiveness within reliable electrolyte systems might enhance the lattice's volumes and compression density within the system as a whole, which contributed to improved ion conduction of solids electrolyte [123–125]. Zhao, Erqing et al. show that PEO-LITFSI-LATP ionic conductivity values of solid electrolytes that have been modified containing LATP nanoparticles calcined as 750°C are 4.02×10^{-4} S/cm and 7.42×10^{-6} S/cm at 55°C and 25°C, correspondingly, as those of solid-state electrolytes reform with LATP nanoparticles heated at 900°C were 4.18×10^{-4} S/cm 4.93×10^{-6} S/cm and at 50°C and 25°C, respectively [126] (Table 3).

Perovskite-type composite polymer electrolyte

Perovskite (ABO_3)-type (A and B are both metal cations) lithium-ion conductivity with structurally associated changes has been identified in the past few years. Several investigations have documented ranging the ionic conductivity

Table 3 The properties of NASICON-based composite-based polymer electrolytes (NCPEs)

Polymer	Lithium salt	LATP (wt%)	Ionic conductivity with temperature	Li^+ trans number	Electrochemical stability (V)	Mechanical strength (MPa)	Ref
PEO	LITFSI	LATP (5wt%)	$9.25\times10^{-6}Scm^{-1}$ at 25°C $5.24\times10^{-4}Scm^{-1}$ at 55°C	–	5	–	[122]
PEO-GF	LITFSI	LATP	$6.3\times10^{-5}Scm^{-1}$ at 25°C	0.37	4.4	33.1	[125]
PAN-PEO	LITFSI	LATP (5wt%)	$5.11\times10^{-4}Scm^{-1}$at 25°C	–	–	–	[126]
		LATP (10wt%)	$8.61\times10^{-4}Scm^{-1}$ at 25°C	–	–	–	
		LATP (20wt%)	$5.34\times10^{-4}Scm^{-1}$ at 25°C	–	–	–	
		LATP (30wt%)	$3.52\times10^{-4}Scm^{-1}$ at 25°C	–	–	–	
PEO	LITFSI	LATP (1wt%)	$6.17\times10^{-6}Scm^{-1}$ at 20°C $1.15\times10^{-5}Scm^{-1}$ at 30°C 1.2×10^{-5} Scm^{-1} at RT	–	–	0.95	[127]
PAN	LITFSI	LATP (10wt%)	$7.89\times10^{-5}Scm^{-1}$ at 25°C	0.33	–	–	[128]
		LATP (20wt%)	$1.05\times10^{-4}Scm^{-1}$ at 25°C				
		LATP (30wt%)	$1.52\times10^{-4}Scm^{-1}$ at 25°C				
		LATP (40wt%)	$1.46\times10^{-4}Scm^{-1}$ at 25°C				
		LATP (50wt%)	$1.42\times10^{-4}Scm^{-1}$ at 25°C				
PVDF-HFP	LITFSI	LATP	2.1×10^{-3} Scm^{-1} at RT	–	–	–	[129]
PEO	$LiClO_4$	LATP (10wt%)	$1.70\times10^{-4}Scm^{-1}$ at 20°C $1.90\times10^{-3}Scm^{-1}$ at 80°C	–	–	–	[130]
PVDF	$LiClO_4$	LATP	$1.76\times10^{-3}Scm^{-1}$ at 20°C	0.74	4.8	3.3	[131]
PEO	LITFSI	LATP (15wt%)	$1.00\times10^{-3}Scm^{-1}$ at 30°C	0.37	5.2	–	[132]
PVDF-HFP	LITFSI	LATP (5wt%)	$4.93\times10^{-5}Scm^{-1}$ at 30°C	–	–	–	[133]
		LATP (10wt%)	$1.11\times10^{-4}Scm^{-1}$ at 30°C				
		LATP (15wt%)	$1.05\times10^{-4}Scm^{-1}$ at 30°C				
		LATP (20wt%)	$7.68\times10^{-5}Scm^{-1}$ at 30°C				
		LATP (25wt%)	$2.63\times10^{-5}Scm^{-1}$ at 30°C				
PEG	LITFSI	LAGP	$6.75\times10^{-5}Scm^{-1}$ at 30°C $3.96\times10^{-4}Scm^{-1}$ at 60°C	0.144	–	–	[134]
PPC	LITFSI	LAGP	~0.56 $mScm^{-1}$	0.77	5	–	[135]
PVDF-HFP	LITFSI	LATP	$3.64\times10^{-3}S$ cm^{-1} RT	0.64	5	–	[136]
PEO	LITFSI	LAGP	1.6×10^{-5} S cm^{-1} RT	–	–	–	[137]
PVDF	LITFSI	LATP	1.64×10^{-3} S cm^{-1} RT	0.45	4.76	14.2	[138]

measurements via switching out of the two s well as B sites by various ions, and with ionized the conductivity values accomplishing 10^{-3} Scm^{-1} (x=0.11) following optimization determined suitable large quantities Li^+ conductive properties' information among different solid electrolytes. The majority of the widespread formulations with a solid-state perovskite-type lithium lanthanum titanate electrolyte were Li_{3x} $La_{(2/3)-x}TiO_3$ (LLTO), using values of x that varied between 0.07 and 0.13 and energies of activation fluctuating around 0.3 to 0.4 eV. The enhanced conductive properties of LLTO ions are attributed to a significant amount of A-site void positions, and researchers have discovered that cationic shortfalls at a location resulting from each of the four neighboring TiO_6 hexagonal shapes may facilitate Li^+ cationic transfers throughout bottlenecks [139–142]. The cations a deficit in the A location reduced monovalent cation conductivity via ions hopping throughout the bottleneck that was generated by the four adjacent nations. BO_6 octahedra compared with LLTO was paired with metallic Li; the conductivity of ions enhanced substantially when compared with blocking electrodes like stainless steel. The ionic transportation boosts as the ambient temperature increases. At increasing temperatures, solid electrolytes showed 2- to 3-fold more substantial conductivity. Doping is also known as additionally enhanced Li-ion propagation by raising the volume of the bottleneck. To boost ionic conductivity, fluoride ion substitution (F for O-2) has further been investigated [143].

The absence of these structures enables monovalent cations that are present to make their way through the barriers generated by the four neighboring BO octahedra. Because the A- and the B-sites in the mentioned framework can tolerate an assortment of ions that have different pleasant states, many investigations upon the effect on the conductivity of ions of the A-site substitutions in $Ln_{0.5}Li_{0.5}TiO_3$ (Ln = La, Pr, Nd, Sm) and the B-site swapping in $Ln_{1/3}Li_xNb_{1-x}$, TiO_3 (Ln = La, Nd) are being carried out and released. The best possible conductivity at regular temperatures is 10^{-3} $\mathrm{s/cm}^{-1}$ [144]. The ionic conductivity of La-doped (LLTO) is lowered; nonetheless, putting La with more significant Sr ions increases the ion conductivity. Consequently, it was recently reported that changing ions that are smaller with La improves A-site area decrease, which leads to reduced constriction sizes throughout lithium-ion movement [145].

Doping, more commonly referred to as the technique, has become increasingly prevalent to improve the general conductivity of LLTO electrolytic membranes. The enhancement in performance may have been attributable to improved bulk conductivity and boosted grain border conductivity or some combination of both. The overall conductivity of Ge-doped LLTO electrolyte membranes (1.2×10^{-5} S cm^{-1}) was a factor of one order of magnitude more substantial than that found in organic LLTO. The all-around conductivity of Zr-doped LLTO (5.84×10^{-5} S cm^{-1}) was approximately 1.9 times that of the undoped specimen. The sort mentioned above of transformation enhanced the overall conductivity alongside the boundary grain conductivity within the electrolyte films [64, 146]. Zhu, Pei, and co-workers investigate PEO/LiTFSI/LLTO solid composite electrolyte ionic conductivity values. The highest value acquired whenever 15 wt% LLTO was introduced to PEO/LiTFSI concrete composite electrolyte at a temperature at room temperature was 2.4×10^{-4} S cm^{-1}. PEO/LiTFSI, PEO/LiTFSI/LLTO (10 wt%), and PEO/LiTFSI/LLTO (20 wt%) composed of solid electrolytes possess ionic conductivity values of 1.75×10^{-5} S cm^{-1}, 6.2×10^{-5} S cm^{-1}, and 5.5×10^{-5} S cm^{-1}, respectfully [147] (Table 4).

Table 4 The properties of perovskite-based composite polymer electrolytes (PCPEs)

Polymer	Lithium salt	Perovskite (wt%)	Ionic conductivity with temperature	Li^+ trans	Electrochemical stability (V)	Mechanical strength (MPa)	Ref
PEO	LiTFSI	LLTO	2.4×10^{-4} S cm^{-1} at RT	–	5.0	–	[147]
PEO	$LiClO_4$	3wt% LLTO	4.01×10^{-4} S cm^{-1} at 60°C	0.15	5.1	–	[148]
			8.42×10^{-4} S cm^{-1} at 80°C	0.19	5.1	–	
PAN	$LiClO_4$	15wt% LLTO	2.4×10^{-4} S cm^{-1} at RT	–	–	–	[149]
PEO	$LiClO_4$	10wt% LLTO	7.99×10^{-4} S cm^{-1} at 70°C	–	–	–	[150]
PEO	$LiClO_4$	10wt% LLTO	2.8×10^{-3} at S cm^{-1} 65°C	–	–	–	[151]
PEO	LiTFSI	5wt% LLTO-nanowires	5.53×10^{-5} S cm^{-1} at RT	–	4.75	–	[152]
			3.63×10^{-4} S cm^{-1} at 60°C				
PEO	LiTFSI	LLTO	1.8×10^{-4} $\mathrm{S\cdot cm}^{-1}$ at RT	–	4.5	–	[153]
PEO	LiTFSI	LLTO	1.43×10^{-4} $\mathrm{S\cdot cm}^{-1}$ at RT	–	4.8	–	[154]
PAN	LiTFSI	LLTO	9.87×10^{-5} $\mathrm{S\cdot cm}^{-1}$ at RT	–	4.8	–	[155]
PEO	LiN $(SO_2CF_2CF_3)_2$	20wt% LLTO	5.0×10^{-4} S/cm at RT	0.7	–	–	[156]

Sulfide-type composite polymer electrolyte

Solid sulfide electrolytes have been gaining prominence because of their high level of conductivity, which renders them analogous to liquid electrolytes. Solid sulfide electrolytes are produced by swapping oxygen-based ions in oxide solid electrolytes with sulfide ions. According to the lower electro-negativity, the amount of interaction involving sulfide and the lithium ions is less than that connecting oxygen and lithium-ion, which therefore could result in a more incredible amount of free-moving lithium ions. Additionally, a sulfide ion's circumference is more significant than an oxygen ion. As a direct consequence, the sulfide solidified electrolyte could offer expanded migration tunnels overall lithium ions, which would prove advantageous for lithium-ion transportation. Due to being at an ambient temperature, solid sulfide electrolytes demonstrate high ionic conductivity values that fluctuate between 10^{-3} and 10^{-4} S cm^{-1} [157–159].

The sulfide-based solid electrolytes are renowned for their helpful lithium-ion conductivity and broad electrochemical windows at ambient temperature. In the meantime, the compressible modulus of sulfide electrolytic is extremely low. Hence, its processing ability is outstanding, indicating that simple freezing may significantly decrease bulk resistivity at ambient temperature. Among the sulfide solid electrolytes, $Li_{9.54}Si_{1.74}P_{1.44}S_{11.7}Cl_{0.3}$ offers the most effective lithium-ion conductivity towards the temperature of the room (25 S/cm), thereby rendering it an ideal application for solid-state Li-based batteries. Nevertheless, the chemical stability could be better and complicate industrial uses of $Li_{9.54}Si_{1.74}P_{1.44}S_{11.7}Cl_{0.3}$ [160]. A nonwoven product the framework has recently been employed for strengthening the sulfide electrolyte which generated thin (70–100 µm) composite material electrolytes alongside moderate ion conductivity (0.1 to 0.3 S cm^{-1}) as well as incorporating an excellent-conductivity sulfide with just a tiny amount of polymer compounds appears to offer a feasible technique for manufacturing thin composite electrolytes membranes that have elevated ionic conductivity; this is accepting that ion percolating is not hampered through the binder [161].

Elimination for crystallization within the polymeric encompassing the nanofiller, modifications in the Li^+ polymer complexity, and improved transport through the surface are the methods used by the sulfide-type solid-state electrolyte for conductivity enhancement. It is particularly mandatory to emphasize that in these composite polymer structures containing different nanoparticles distributed in a polymer matrix, the ceramic's fillers primarily enhance the conductivity within the polymer's phases [162]. Nevertheless, making use of sulfide solid electrolytes continues to confront two significant obstacles: (1) chemical imbalance in the atmosphere caused by aqueous hydrolysis and (2) electromechanical instability using metal Li anode and oxide cathode components [163, 164]. The composite electrolytes encompassing $LiSn_2(PO_4)_3$ (LSP) wt. 30% PEO+$LiClO_4$ show a maximum ionic conductivity of 3.48×10^{-5} Scm^{-1} at 27°C, resulting in maximization to 1.18×10^{-4} Scm^{-1} at 60°C. The less activation energy of 0.34 eV results from greater lithium-ion mobility in a composite electrolyte [165] (Table 5).

Table 5 The properties of sulfide-based composite-based polymer electrolytes (SCPEs)

Polymer	Lithium salt	Sulfide (wt%)	Ionic conductivity with temperature	Li^+ trans	Electrochemical stability (V)	Mechanical strength (MPa)	Ref
PVDF-HFP	LiTFSI	LiPS	1.1×10^{-4} S cm^{-1} at RT	–	–	–	[166]
PVDFHFP/ PFPEs	LiTFSI	20 wt% LGPS	0.18 mS cm^{-1} at 25°C	0.68	4.86	–	[167]
PVDF	LiTFSI	LPS	3.42×10^{-4} S/cm at RT	0.44	–	–	[168]
PEO	LiTFSI	LGPS	4.38×10^{-7} S cm^{-1} at 20°C	–	–	–	[169]
PEO	LiTFSI	1 wt% LGPS	1.21×10^{-3} S cm^{-1} at 80°C 1.18×10^{-5} S cm^{-1} at 25°C		5.67	–	[170]
PEO	LiTFSI	1 wt% LGPS	9.10×10^{-5} S cm^{-1} at 25°C	–	5.5	–	[171]
PEO	LiTFSI	LPS	8.01×10^{-4} S cm^{-1} at 60°C	–	5.1	–	[172]
PEO	LiTFSI	1Wt% LSPS	1.69×10^{-4} S cm^{-1} at 60°C	–	–	–	[173]
PEO	LiTFSI	5 Wt% LSPS	5.31×10^{-4} S cm^{-1} at RT	–	–	–	[174]
PVDF	LiTFSI	5 Wt% LSPS	4.54×10^{-4} S cm^{-1} at RT	–	–	–	
PVDF	LiTFSI	3 Wt% LSPS	7.07×10^{-4} S cm^{-1} at RT	–	–	–	
PEO	$LiClO_4$	LSP	3.48×10^{-5} Scm^{-1} at 27 °C 1.18×10^{-4} Scm^{-1} at 60 °C 3.48×10^{-5} Scm^{-1} at RT	0.39	–	–	[175]

Inactive fillers

In general, inactive particle fillers fall into two groups: metal oxide ceramic particles (Al_2O_3, MgO_2, TiO_2, and SiO_2) and ferroelectric ceramic particles ($BaTiO_3$, $PbTiO_3$, and $SrBi_4Ti_4O_{15}$) [17]. The incorporation of nano-sized passive (or) inactive filler raised the Lewis-acid-based relationship that existed between the polarized function categories located on the filler's surfaces and the ions in the charged particles, establishing an area for the transfer of charge translocation, which improved the mobility of ions and conductive properties. Due to their high dielectric value and separation of charges, ferroelectric ceramic fillers are used to enhance membrane polarization. The ion's conductivity and Li^+ interaction durability are improved by reinforcing polymeric amorphous areas [8, 176, 177]. Inactive additives incorporated into a PEO-based polymer matrix can change crystallization dynamics by adding local unstructured areas at the filler-polymer interaction. The density of entanglement in the amorphous space increases by constructing network nodes at the filler-polymer interface, resulting in improved mechanical properties of the materials. Li^+ migration effectiveness is improved, leading to more excellent Li^+ conduction [178].

Incorporating silicon dioxide, also known as SiO_2, in polymeric electrolytes was discovered to increase ionic conductivity, leading to greater interfacial, mechanical, and thermal distinctive features. The silica nanoparticles have a high surface-to-volume proportion, and Si–O–Si chains communicate with functional polymer groups, resulting in additional ion dissociation and improving ionic conductivity. Incorporating nonconducting silica nanoparticles with high concentrations could restrict the effective surface area between the electrode-electrolyte contact and affect the conductivity of ions [179]. However, a significant SiO_2 loading, on the other hand, may produce agglomerate and pulverization, which cause lagging kinetics. Likewise, using SiO_2 nanoparticles within a polymer solution could result in agglomeration and particle formation throughout the process, resulting in poor cycle efficiency [180].

Several include the more effective thermal, mechanical, and chemical capabilities, and also, because of its high surface area, titanium dioxide (TiO_2) is a suitable option for emerging technological innovations [181]. The $PbTiO_3$ (lead titanate) is a perovskite that exhibits a distorted tetragonal phase. Physical filler infiltration through the polymer's hosting is commonly utilized to reduce crystallinity, promote physical durability, and increase electrolyte absorption in the solution [14]. The nanocomposite polymer electrolyte (NCPE) is primarily produced by combining metal oxides, including TiO_2, SiO_2, Al_2O_3, and ZrO_2, and the aluminates and titanates. Even small quantities of these fillers might have affected polymer electrolytes' mechanical strength and ion conductivity. The enhanced ionic conductivity of NCPEs is influenced by various factors, including the function of ceramics filler as a kind of solid plasticizer [182–185] (Table 6).

Synthesis methods for composite polymer electrolyte preparation

The nanocomposites of polymers are produced through a wide range of methodologies, among them the solution cast technique, in situ polymerization technique, melt intercalation technique, spin coating technique, hot press technique, and dip coating technique.

Solution cast technique

Due to the convenience of manufacturing, it is the most common technique for manufacturing films from polymers of different thicknesses (50–300 µm). In the beginning, by continuous stirring, the necessary quantity of polymer host dissolves in the acceptable solvent. A desired amount of salt is subsequently added to the homogenous polymeric matrix and is stirred again until a homogeneous and homogeneous solution appears. For polymer nanocomposite production, a nanoparticle is initially mixed with the solvent before ultrasonication is employed to enhance the dispersion. The resulting solution is subsequently added to the polymer solution containing salt and stirred until the solution turns homogeneous. Subsequently, the viscous solutions are cast in a petri dish and kept at ambient temperature to allow the solvent to evaporate. Finally, the viscous solution is cast in a petri dish and kept at room temperature to allow the solvent to evaporate. The petri dish is subsequently placed in an oven under a vacuum to remove the remaining solvent, and the protective film gets peeled off [192–195] (Fig. 9).

Melt intercalation technique

This technology is fundamental because it helps protect the environment, is cost-effective, and does not require solvents. It is worth noting that optimizing the heat properties is necessary to improve how particles spread out, as extreme temperatures can change the surface properties of nanoparticles and cause them to break down. The process starts with heating the polymer matrix at a temperature. Then, add the nanoparticles

Table 6 The properties of inactive fillers -based composite-based polymer electrolytes

Polymer	Lithium salt	Inactive filler	Ionic conductivity with temperature	Li^+ trans	Electrochemical stability (V)	Mechanical strength (MPa)	Ref
PEO	LiTFSI	SiO_2	3.3×10^{-4} Scm^{-1} at 60°C	–	–	–	[180]
PMMA	$LiClO_4$	TiO_2	3×10^{-4} S/cm at 303 K	–	–	–	[181]
PVA: PVdF	$LiCF_3SO_3$	TiO_2	3.7×10^{-3} Scm^{-1} at 303 K	–	–	22.6	[178]
PAN	$LiClO_4$	Al_2O_3	5.71×10^{-4} S/cm at RT	–	–	–	[182]
PEO: PMMA	LiTFSI	Al_2O_3	9.39×10^{-7} at S/cm at RT	–	4.9	–	[183]
P(VdF-HFP)	$LiClO_4$	CeO_2	3.84mS·cm^{-1}at RT	–	4.8	–	[184]
PEO	LiTFSI	Ca–CeO_2	1.3×10^{-4} S cm^{-1}at 60 °C	0.45	–	–	[185]
P(VdF-HFP)	$LiClO_4$	MgO	7.63×10^{-3} Scm^{-1} at RT	–	5.0	–	[186]
PEMA/PVA	$LiClO_4$	TiO_2	$2.745\times10^{-3}$$Scm^{-1}$ at RT	–	–	–	[187]
PVDF–HFP/TPU/PMMA	$LiClO_4$	SiO_2	8.5 $\times10^{-3}$ Scm^{-1} at RT	–	5.9	10.6	[188]
PEO/PVDF	$LiClO_4$	$BaTiO_3$	1.2×10^{-4} S/cm at RT	–	–	–	[189]
PEO	LiTFSI	$BaTiO_3$	5.83×10^{-5} Scm^{-1}at 30°C	–	5.8	–	[180]
PMMA	$LiClO_4$	MgO	8.14×10^{-3} S cm^{-1} at RT	–	5.1	–	[190]
PEO	$LiClO_4$	Zno	6.33×10^{-5} S cm^{-1} at RT	–	–	–	[191]
PEO–PMMA	$LiClO_4$	SiO_2	0.51×10^{-5} S cm^{-1} at RT	0.989	–	–	[176]
		Al_2O_3	0.38×10^{-5} S cm^{-1} at RT	0.983	–	–	
		ZnO	1.67×10^{-5} S cm^{-1} at RT	0.985	–	–	
		SnO_2	1.00×10^{-5} S cm^{-1} at RT	0.988	–	–	

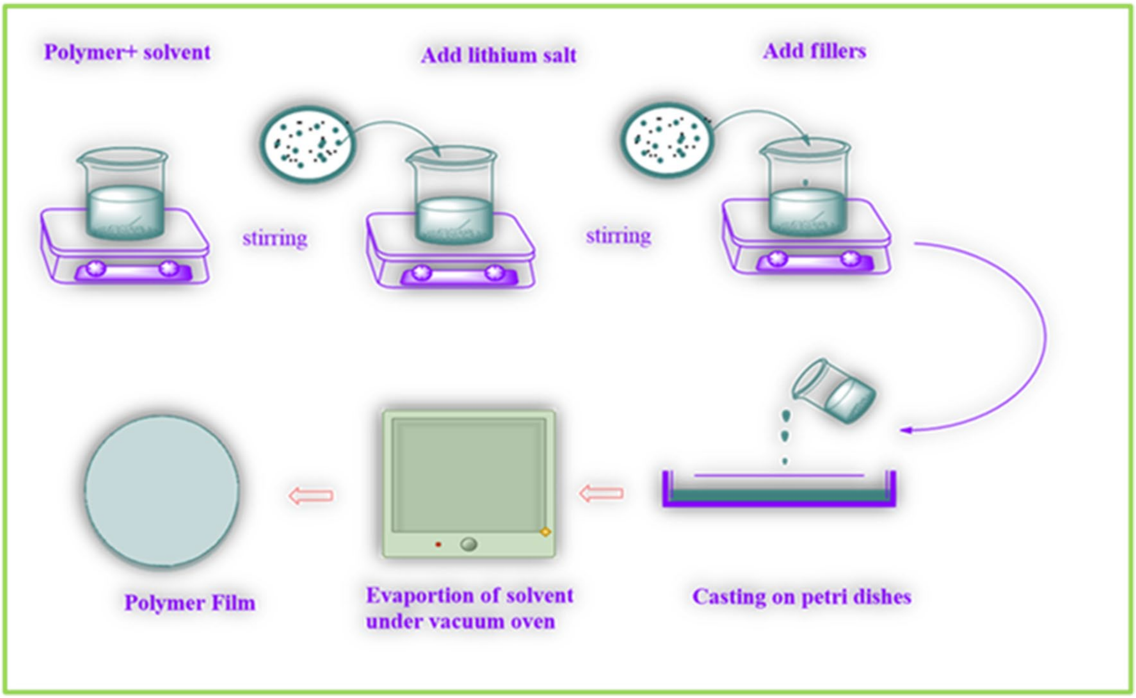

Fig. 9 The preparation of the solution casting technique

while carefully mixing everything to ensure an even distribution. In addition, how the clay/nanofiller is modified on its surface, how it interacts with the polymers it is mixed, and various manufacturing factors all play a role, in how the nanoparticles are dispersed throughout [196–199] (Fig. 10).

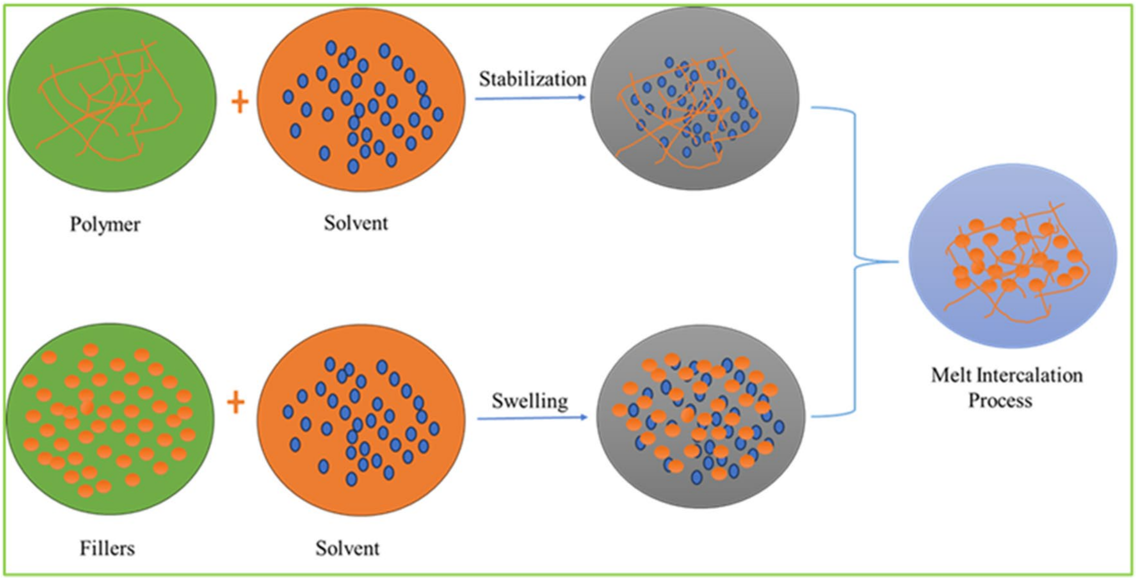

Fig. 10 The preparation of the melt intercalation technique

Spin coating technique

The technique is identical to the solution cast method. The primary advantages of the spin coating method are its simplicity and relative ease of preparation, and it produces homogeneity thicknesses varying from a few nanometers to a few microns. A small solution is set on a substrate and then placed on the spin coater, which may revolve at the required speed. The spreads get spread on a substrate by centrifuge followed by heating that evaporates the solvent from the surface. To be coated, the substrate's rotating axis must be perpendicular to the substrates. The overall thickness of the film is influenced by (i) the viscosity of the mixture, (ii) the level of concentration of the mixture, (iii) the rotational speed, and (iv) the spin. Fortunately, this technique is only beneficial for extremely viscous mixes rather than particularly high-viscosity mixtures. The spin coater rotation is unsuitable for distributing the mixture droplet to produce a thin film in a gel-like mixture [200–202] (Fig 11).

Hot press technique

The hot press technique is distinctive because it is low cost, is solvent-free, generates an excellent film with thick materials, and offers a quicker strategy. The setup contains a weighing cylinder, a heating chamber, a basement, and a temperature controller.

Initially, the polymer, the salt, and the nanoparticle are crushed for the desired amount of time in the agate mortar. The manufactured mixture is subsequently heated (to close

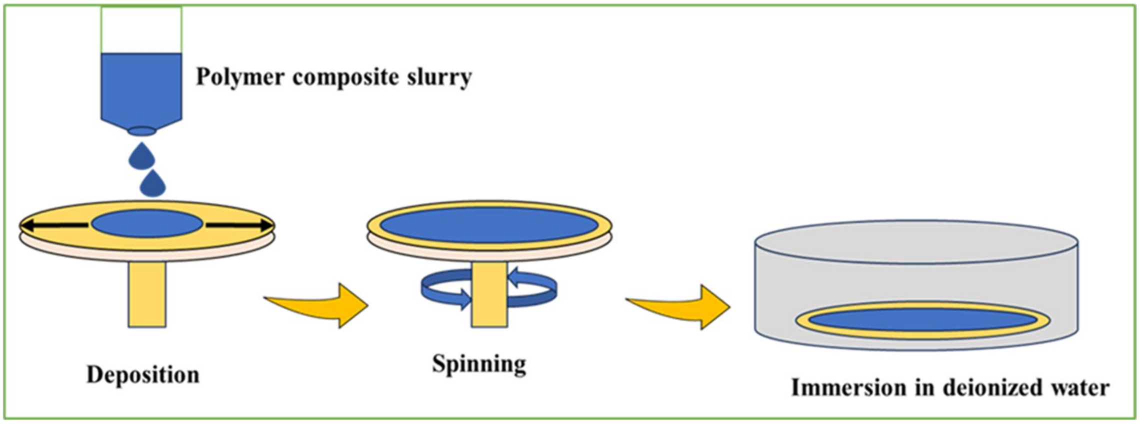

Fig. 11 The preparation of the spin coating technique

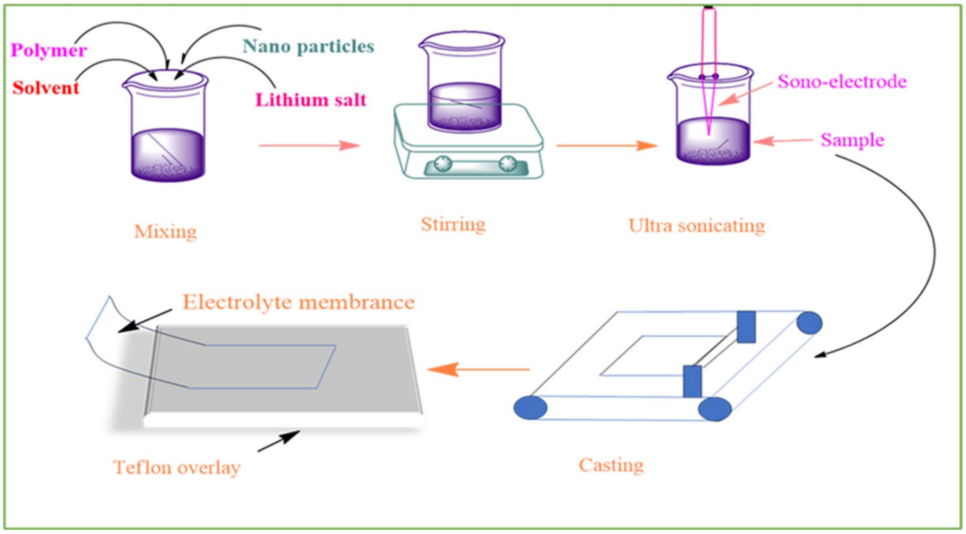

Fig. 12 The preparation of the hot press technique

to the polymer melting point), and the slurry that emerges is then sandwiched between the stainless-steel (SS) blocks. The mixture is followed by pressing pressure-controlled equipment, and the resulting film is utilized for further characterization [203, 204] (Fig. 12).

Dip coating

The unique characteristic of dip coating is that it makes it possible for us to get excellent quality film on both sides of the substrates despite becoming a low-cost procedure. In the beginning, the chosen substrates are immersed in the solvent. In a three-step process, solvent evaporation is followed by immersion, deposition, and drainage. In immersion, the substrate is submerged in solution at a pace that allows sufficient time for coating. In the phases that follow phase, deposition, and drainage, the substrate is immersed in the solvent for a sufficient amount of time to allow the substrate to interact with the solvent. The substrate is now progressively drawn out at an even rate, which causes the creation of a thin coating on the substrate. In the final phase of evaporation, the solution of the solvent has evaporated, and the substrate may be warmed to eliminate any remaining solvent. The speed of elimination and the density of the resulting solution can be utilized to modify the thickness and quality of the film [205–208], (Fig 13).

Strategies and outlooks of the performance of composite polymer electrolytes

CPEs have been receiving ample attention in recent years as potential possibilities to improve further the performance of lithium-ion rechargeable batteries (LIBs) and

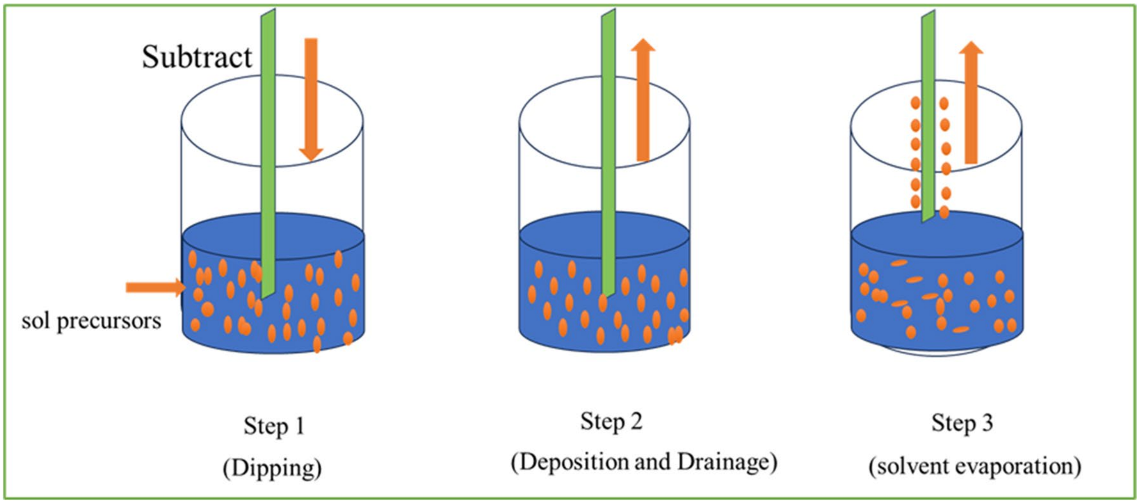

Fig. 13 The preparation of the dip coating technique

lithium-metal batteries (LMBs)…etc. These substances incorporate the beneficial properties of solid electrolytes having polymers, intending to boost the security, stability, and general effectiveness of lithium-based battery packs. Several techniques and opportunities could enhance composite polymer electrolytes using lithium-based batteries. Here are some strategies and outlooks to consider for improving their performance

Polymer matrix selection

Identify a polymer matrix with excellent conductivity of ions, mechanical strength, and thermal stability. As a result of the ability, they have to communicate with the ions of lithium while providing mechanical solid properties; polymers that react, such as polyethylene oxide (PEO), polypropylene oxide (PPO), polyacrylonitrile (PAN), and the corresponding derivatives are often utilized.

Enhancing ionic conductivity

Ceramic filler incorporation Including ceramic additives that include oxides or sulfide nanomaterials through the matrix of polymers could enhance the conductivity of ions within the composite electrolyte. These additives provide pathways for lithium-ion transportation, reducing the overall resistance.

Nanostructured materials Utilizing nanoscale substances, nano-sized particles, or nanofibers, nanowires can increase surface area and accelerate lithium-ion transport, raising a whole conductivity.

Improved electrochemical stability

Electrolyte additives Incorporating additives that produce stable passivation layers on the electrode surfaces may be beneficial in slowing down the degradation of the two components of the composite electrolyte and the electrodes themselves. These modifications boost a battery's long-term reliability.

Cross-linking polymers The cross-linking chains of polymers may enhance the electrolyte's mechanical and chemical stability. This minimizes the possibility of dendritic development, circumvents leakage, and improves cycle endurance in lithium-ion batteries.

Mechanical properties

Flexibility and stretchability Constructing composite polymer electrolytes with improved mechanical properties permits them to maintain their stability when they are challenged by mechanical strain or deformations. This feature is especially essential for flexible and wearable battery storage devices.

Electrode-electrolyte interface

The relationship between the solid electrolyte and an electrode is essential in ensuring the general operation of the batteries. Composite polymer electrolytes can be generated to enhance wetting and interaction with the electrode components. This may increase charging and discharging accelerates by minimizing interface impedance.

Safety

Nonflammability Although polymeric electrolytes are generally not flammable, presenting flame-resistant substances may enhance the protection of composite electrolyte polymers.

Suppression of dendrite formation For the prevention of shorts in electrical circuits and thermal runaway in lithium-metal battery packs, it is essential to avoid the formation of lithium dendrites; the purpose of preventing dendrite formation, composite electrolytes may supply support by mechanical means.

Synthesis and manufacturing

Scalability Subsequently, it is of the utmost importance for the creation of methods for synthesis that can be sustainable using massive operations manufacturing methods to go from laboratory-scale research to manufacturing for commercial use. Developing sustainable and inexpensive methods for depositing the composite electrolyte upon materials for electrodes, which might include solution casting, electrospinning, or inkjet printers, will improve manufacturing possible production.

Solvent-free fabrication Solvent-free technologies, including solid-state blending or melting processing, may mitigate solvent-related obstacles while simplifying manufacture.

Conclusion

CPEs help boost electrochemical systems' functioning, including batteries and fuel cell systems. Finally, the subsequent essential characteristics of composite polymer electrolytes could be summarized as follows.

Ionic conductivity CPEs demonstrate more excellent conductivity of ions than conventional electrolytic polymers. The room-temperature (RT) ionic conductivity of most active fillers stays in the 10^{-4} Scm^{-1} order of magnitude, with just a few achieving values close to 10^{-3} Scm^{-1}. At room temperature, passive fillers have a low ionic conductivity of 10^{-6} to 10^{-5} S cm^{-1} or even much lower. In practice, however, the ionic conductivity of solid-state electrolytes has been calculated to be 10^{-3} S cm^{-1}. The mechanism of ionic transportation in composite polymer electrolytes is still being investigated thoroughly, which is the most significant impediment to achieving the requisite degree of ionic conductivity. Consequently, it becomes essential to comprehend the transportation mechanism of Li-ions in CPEs along with the enhancement process of inorganic additives in ion conductivity.

Mechanical stability Using inorganic additions enhances the tensile strength and endurance of CPEs, decreasing problems such as bloating and leakage that can occur with pure polymer electrolytes. This advancement is consistent with the safe and reliable operation of electrochemical equipment. To maximize the effectiveness of processing and physical, chemical, and electromechanical compatibility with both the anode and cathode electrodes, the mechanical strength and thermal stability of CPEs must be significantly expanded since their performance is closely dependent upon the safety of batteries.

Wide electrochemical stability window The ESW is the voltage difference between the oxidation and reduction potentials of the electrolyte. CPE electrochemical stability could be substantially upgraded. CPEs' electrochemical stability window determines which could be connected with high-voltage electrode materials. On the other hand, the interaction between the electrochemical stability of the CPEs and electrode components has an essential influence on battery cycling stability. The required electromechanical stability window for polymer electrolytes of 5 to 5.5 V (versus Li/Li^+) is suitable for practical application.

Interface stability Incorporating inorganic filler substances in CPE composite electrolytes of polymers may enhance the interface stability between the electrode and electrolyte surfaces, minimizing side reactions and expanding general device efficiency and lifespan. Interface stability in CPEs significantly impacts the performance and long-term viability of various electrochemical appliances, such as fuel cells, rechargeable batteries, and supercapacitors. To enhance ions' conductivity and physical properties, active fillers such as nanoparticles or similar conducting components can be established in polymeric electrolytes. It is essential to maintain the overall performance and durability of the CPEs by ensuring the interface stability between their polymer matrix and these active fillers.

Li^+ transfer number The transferred ratio is quite close to 1 for lithium-ion batteries. This suggests that practically all of the lithium ions in the battery play a role in the electrochemical events. Active filler-based composite polymer electrolytes have a significantly higher lithium transference number (Li^+) (0.9 vs. 0.5) than passive filler-based composite polymer electrolytes. One of the most significant advantages of lithium-ion batteries is their high transfer number, which allows for fast charging and draining.

Future challenges The relevance of the apparent benefits of maximizing the performance of CPEs remains challenging. Among them are preserving ion conductivity while preserving mechanical stiffness, reducing interface resistance, and addressing filler dispersion and aggregation difficulties. More investigation must be conducted to tackle the obstacles to ultimately fulfilling the CPE's promise.

Composite polymer electrolytes have many opportunities for creative ideas for polymers for electrochemical devices since they have boosted ion conductivity, mechanical durability, electromechanical stability, interfacial stability, and adaptability. Continuous advancement and study improvements must continue to solve remaining problems and enhance the effectiveness of CPEs employed to provide valuable recommendations. The concept is to continuously determine the combinations and interactions of SPEs and inorganic fillers. Overall, CPEs indicate promising potential for real-world applications in the foreseeable future.

Supplementary Information The online version contains supplementary material available at https://doi.org/10.1007/s11581-023-05318-y.

Acknowledgements The authors would like to express their gratitude and sincere appreciation to the Vellore Institute of Technology.

Author contribution M. Jagan: methodology, investigation, formal analysis, writing—original draft. S.P. Vijayachamundeeswari: resources, validation, formal analysis, supervision, resources, validation, visualization, writing—review and editing. All authors reviewed the manuscript.

Data availability The data that support the findings of this study are available from the corresponding author upon reasonable request.

Declarations

Conflict of interest The authors declare no competing interests.

References

1. Vickraman P, Reddy BJ (2019) Performance of ferrocyanic PVDF-co-HEP micro composite electrolytes cum separators for Li-ion batteries. AIP Conf Proc 2115

2. Hu XL, Hou GM, Zhang MQ, Rong MZ, Ruan WH, Giannelis EP (2012) A new nanocomposite polymer electrolyte based on poly (vinyl alcohol) incorporating hyper grafted nano-silica. J Mater Chem 22(36):18961–18967
3. Armand M, Tarascon JM (2008) Building better batteries. Nature 451(7179):652–657
4. Goodenough JB (2015) Energy storage materials: a perspective. Energy Storage Mater:158–161
5. Li X, Wang Y, Xi K, Yu W, Feng J, Gao G, Wu H, Jiang Q, Abdelkader A, Hua W, Zhong G (2022) Quasi-solid-state ion-conducting arrays composite electrolytes with fast ion transport vertical-aligned interfaces for all-weather practical lithium-metal batteries. Nanomicro Lett 14(1):210
6. Chew KW, Ng TC, How ZH (2013) Conductivity and microstructure study of PLA-based polymer electrolyte salted with lithium perchloride, LiClO4. Int J Electrochem Sci 8(5)
7. Verma ML, Sahu HD (2017) Study on ionic conductivity and dielectric properties of PEO-based solid nanocomposite polymer electrolytes. Ionics 23(9):2339–2350
8. Zhou D, Shanmukaraj D, Tkacheva A, Armand M, Wang G (2019) Polymer electrolytes for lithium-based batteries: advances and prospects. Chem 5(9):2326–2352
9. Pandurangan S, Kaliyappan K, Ramaswamy AP, Ramaswamy M (2021) Polymer-garnet composite electrolyte based on comb-like structured polymer for lithium-metal batteries. Mater Today Energy 21:100836
10. Yao P, Yu H, Ding Z, Liu Y, Lu J, Lavorgna M, Wu J, Liu X (2019) Review on polymer-based composite electrolytes for lithium batteries. Front Chem 7:522
11. Ding WQ, Lv F, Xu N, Wu MT, Liu J, Gao XP (2021) Polyethylene oxide-based solid-state composite polymer electrolytes for rechargeable lithium batteries. ACS Appl Energy Mater 4(5):4581–4601
12. Merrill LC, Chen XC, Zhang Y, Ford HO, Lou K, Zhang Y, Yang G, Wang Y, Wang Y, Schaefer JL, Dudney NJ (2020) Polymer–ceramic composite electrolytes for lithium batteries: a comparison between the single-ion-conducting polymer matrix and its counterpart. ACS Appl Energy Mater 3(9):8871–8881
13. Gagliardi GG, Ibrahim A, Borello D, El-Kharouf A (2020) Composite polymers development and application for polymer electrolyte membrane technologies—a review. Molecules 25(7):1712
14. Zeis R (2015) Materials and characterization techniques for high-temperature polymer electrolyte membrane fuel cells. Beilstein J Nanotechnol 6(1):68–83
15. Zhou Z, Zholobko O, Wu XF, Aulich T, Thakare J, Hurley J (2020) Polybenzimidazole-based polymer electrolyte membranes for high-temperature fuel cells: current status and prospects. Energies 14(1):135
16. Yusoff NF, Idris N (2017) Ionic liquid based PVDF/PMMA gel polymer electrolyte for lithium rechargeable battery. J Mech Eng Sci 11:3152–3165
17. Akitomo F, Sasabe T, Yoshida T, Naito H, Kawamura K, Hirai S (2019) Investigation of effects of high temperature and pressure on a polymer electrolyte fuel cell with polarization analysis and X-ray imaging of liquid water. J Power Sources 431:205–209
18. Li Y, Zhang W, Dou Q, Wong KW, Ng KM (2019) Li 7 La 3 Zr 2 O 12 ceramic nanofiber-incorporated composite polymer electrolytes for lithium metal batteries. J Mater Chem A 7(7):3391–3398
19. Li Z, Huang HM, Zhu JK, Wu JF, Yang H, Wei L, Guo X (2018) Ionic conduction in composite polymer electrolytes: case of PEO: Ga-LLZO composites. ACS Appl Mater Interfaces 11(1):784–791
20. Fu J, Li Z, Zhou X, Guo X (2022) Ion transport in composite polymer electrolytes. Mater Adv 3(9):3809–3819
21. Lagadec MF, Zahn R, Wood V (2019) Characterization and performance evaluation of lithium-ion battery separators. Nat Energy 4(1):16–25
22. Commarieu B, Paolella A, Daigle JC, Zaghib K (2018) Toward high lithium conduction in solid polymer and polymer–ceramic batteries. Curr Opinion Electrochem 9:56–63
23. Zhang H, Li C, Piszcz M, Coya E, Rojo T, Rodriguez-Martinez LM, Armand M, Zhou Z (2017) Single lithium-ion conducting solid polymer electrolytes: advances and perspectives. Chem Soc Rev 46(3):797–815
24. Yang H, Wu N (2022) Ionic conductivity and ion transport mechanisms of solid-state lithium-ion battery electrolytes: a review. Energy Sci Eng 0(5):1643–1671
25. Yang X, Liu J, Pei N, Chen Z, Li R, Fu L, Zhang P, Zhao J (2023) The critical role of fillers in composite polymer electrolytes for a lithium battery. Nanomicro Lett 15(1):1–37
26. Wang W, Alexandridis P (2016) Composite polymer electrolytes: nanoparticles affect structure and properties. Polymers 8(11):387
27. Li S, Yang B, Wang C, Wang J, Feng Y, Yan B, Xiong Z, Du Y (2017) A facile and green fabrication of Cu2O-Au/NG nanocomposites for sensitive electrochemical determination of rutin. J Electroanal Chem 786:20–27
28. Fan LZ, He H, Nan CW (2021) Tailoring inorganic–polymer composites for the mass production of solid-state batteries. Nat Rev Mater 6(11):1003–1019
29. Liu C, Wang J, Kou W, Yang Z, Zhai P, Liu Y, Wu W, Wang J (2021) A flexible, ion-conducting solid electrolyte with vertically bicontinuous transfer channels toward high-performance all-solid-state lithium batteries. Chem Eng J 404:126517
30. Lu Z, Peng L, Rong Y, Wang E, Shi R, Yang H, Xu Y, Yang R, Jin C (2022) Enhanced electrochemical properties and optimized Li+ transmission pathways of PEO/LLZTO-based composite electrolytes modified by supramolecular combination. Energy Environ Mater:12498
31. Huo S, Sheng L, Xue W, Wang L, Xu H, Zhang H, He X (2013) Challenges of polymer electrolyte with wide electrochemical window for high energy solid-state lithium batteries. Info Mat 5(3):12394
32. Chen L, Li Y, Li SP, Fan LZ, Nan CW, Goodenough JB (2018) PEO/garnet composite electrolytes for solid-state lithium batteries: From "ceramic-in-polymer" to "polymer-in-ceramic". Nano Energy 46:176–184
33. Szczęsna-Chrzan A, Marczewski M, Syzdek J, Kochaniec MK, Smoliński M, Marcinek M (2023) Lithium polymer electrolytes for novel batteries application: the review perspective. Appl Phys A 129(1):37
34. Zhang X, Liu T, Zhang S, Huang X, Xu B, Lin Y, Xu B, Li L, Nan CW, Shen Y (2017) Synergistic coupling between Li6. 75La3Zr1. 75Ta0. 25O12 and poly (vinylidene fluoride) induce high ionic conductivity, mechanical strength, and thermal stability of solid composite electrolytes. J Am Chem Soc 139(39):13779–13785
35. Sun C, Liu J, Gong Y, Wilkinson DP, Zhang J (2017) Recent advances in all-solid-state rechargeable lithium batteries. Nano Energy 33:363–386
36. Zhang B, Tan R, Yang L, Zheng J, Zhang K, Mo S, Lin Z, Pan F (2018) Mechanisms and properties of ion-transport in inorganic solid electrolytes. Energy Stor Mater 10:139–159
37. Long L, Wang S, Xiao M, Meng Y (2016) Polymer electrolytes for lithium polymer batteries. J Mater Chem A 4(26):10038–10069
38. Xue Z, He D, Xie X (2015) Poly (ethylene oxide)-based electrolytes for lithium-ion batteries. J Mater Chem A 3(38):19218–19253

39. Yang Q, Wang A, Luo J, Tang W (2022) Improving ionic conductivity of polymer-based solid electrolytes for lithium metal batteries. Chin J Chem Eng 43:202–215
40. Zhang D, Meng X, Hou W, Hu W, Mo J, Yang T, Zhang W, Fan Q, Liu L, Jiang B, Chu L (2023) Solid polymer electrolytes: ion conduction mechanisms and enhancement strategies. Nano Res Energy 2(2):e9120050
41. Yang X, Liu J, Pei N, Chen Z, Li R, Fu L, Zhang P, Zhao J (2023) The critical role of fillers in composite polymer electrolytes for lithium battery. Nanomicro Lett 15(1):74
42. Borodin O, Smith GD (2006) Mechanism of ion transport in amorphous poly (ethylene oxide)/LiTFSI from molecular dynamics simulations. Macromolecules 39(4):1620–1629
43. Mao G, Perea RF, Howells WS, Price DL, Saboungi ML (2000) Relaxation in polymer electrolytes on the nanosecond timescale. Nature 405(6783):163–165
44. Aziz SB, Woo TJ, Kadir MF, Ahmed HM (2018) A conceptual review on polymer electrolytes and ion transport models. J Sci Adv Mater Dev 3(1):1–7
45. Ratner MA, Johansson P, Shriver DF (2000) Polymer electrolytes: ionic transport mechanisms and relaxation coupling. Mrs Bull 25(3):31–37
46. Utpalla P, Sharma SK, Sudarshan K, Deshpande SK, Sahu M, Pujari PK (2020) Investigating the correlation of segmental dynamics, free volume characteristics, and ionic conductivity in poly (ethylene oxide)-based electrolyte: a broadband dielectric and positron annihilation spectroscopy study. J Phys Chem C 124(8):4489–4501
47. Devaux D, Bouchet R, Glé D, Denoyel RJ (2012) Mechanism of ion transport in PEO/LiTFSI complexes: effect of temperature, molecular weight, and end groups. Solid State Ion 227:119–127
48. Williams ML, Landel RF, Ferry JD (1955) The temperature dependence of relaxation mechanisms in amorphous polymers and other glass-forming liquids. J Am Chem Soc 77(14):3701–3717
49. Arya A, Sharma AL (2017) Polymer electrolytes for lithium-ion batteries: a critical study. Ionics 23(3):497–540
50. Shukla N, Thakur AK, Shukla A, Marx DT (2014) Ion conduction mechanism in solid polymer electrolyte: applicability of almond-west formalism. Int J Electrochem Sci9(12):7644-7659
51. Xu J (2022) critical review on cathode–electrolyte interphase toward high-voltage cathodes for Li-ion batteries. Nano Lett 14(1):166
52. Gao Y, Zhang B (2023) Probing the mechanically stable solid electrolyte interphase and the implications in design strategies. Adv Mater 35(18):2205421
53. Maurya DK, Dhanusuraman R, Guo Z, Angaiah S (2022) Composite polymer electrolytes: progress, challenges, and future outlook for sodium-ion batteries. Adv Compos Hybrid Mater 5(4):2651–2674
54. Chen R, Qu W, Guo X, Li L, Wu F (2016) The pursuit of solid-state electrolytes for lithium batteries: from comprehensive insight to emerging horizons. Mater Horiz 3(6):487–516
55. Liu S, Liu W, Ba D, Zhao Y, Ye Y, Li Y, Liu J (2023) Filler-integrated composite polymer electrolyte for solid-state lithium batteries. Adv Mater 35(2):2110423
56. Zhou Q, Ma J, Dong S, Li X, Cui G (2019) Intermolecular chemistry in solid polymer electrolytes for high-energy-density lithium batteries. Adv Mater 31(50):1902029
57. Xu S, Hu L (2020) Towards a high-performance garnet-based solid-state Li metal battery: a perspective on recent advances. J Power Sources 472:228571
58. Wan Z, Lei D, Yang W, Liu C, Shi K, Hao X, Shen L, Lv W, Li B, Yang QH, Kang F (2019) Low resistance–integrated all-solid-state battery achieved by Li7La3Zr2O12 nanowire upgrading polyethylene oxide (PEO) composite electrolyte and PEO cathode binder. Adv Funct Mater 29(1):1805301
59. Tao X, Liu Y, Liu W, Zhou G, Zhao J, Lin D, Zu C, Sheng O, Zhang W, Lee HW, Cui Y (2017) Solid-state lithium–sulfur batteries operated at 37 C with composites of nanostructured Li7La3Zr2O12/carbon foam and polymer. Nano Lett 17(5):2967–2972
60. Liang JY, Zeng XX, Zhang XD, Wang PF, Ma JY, Yin YX, Wu XW, Guo YG, Wan LJ (2018) Mitigating interfacial potential drop of cathode–solid electrolyte via ionic conductor layer to enhance interface dynamics for solid batteries. J Am Chem Soc 140(22):6767–6770
61. Song X, Wang C, Chen J, Xin S, Yuan D, Wang Y, Dong K, Yang L, Wang G, Zhang H, Zhang S (2022) Unraveling the synergistic coupling mechanism of Li+ transport in an “ionogel-in-ceramic” hybrid solid electrolyte for rechargeable lithium metal battery. Adv Funct Mater 32(10):2108706
62. Zhang J, Zang X, Wen H, Dong T, Chai J, Li Y, Chen B, Zhao J, Dong S, Ma J, Yue L (2017) High-voltage and free-standing poly (propylene carbonate)/Li 6.75 La 3 Zr 1.75 Ta 0.25 O 12 composite solid electrolyte for wide temperature range and flexible solid lithium-ion battery. J Mater Chem A 5(10):4940–4948
63. Zhao CZ, Zhang XQ, Cheng XB, Zhang R, Xu R, Chen PY, Peng HJ, Huang JQ, Zhang Q (2017) An anion-immobilized composite electrolyte for dendrite-free lithium metal anodes. Proc Natl Acad Sci 114(42):11069–11074
64. Liu W, Liu N, Sun J, Hsu PC, Li Y, Lee HW, Cui Y (2015) Ionic conductivity enhancement of polymer electrolytes with ceramic nanowire fillers. Nano Lett 15(4):2740–2745
65. Dong W, Zeng XX, Zhang XD, Li JY, Shi JL, Xiao Y, Shi Y, Wen R, Yin YX, Wang TS, Wang CR (2018) Gradiently polymerized solid electrolyte meets with micro-/nanostructured cathode array. ACS Appl Mater Interfaces 10(21):18005–18011
66. Xin S, You Y, Wang S, Gao HC, Yin YX, Guo YG (2017) Solid-state lithium metal batteries promoted by nanotechnology: progress and prospects. ACS Energy Lett 2(6):1385–1394
67. Lin D, Liu W, Liu Y, Lee HR, Hsu PC, Liu K, Cui Y (2016) High ionic conductivity of composite solid polymer electrolyte via in situ synthesis of monodispersed SiO2 nanospheres in poly (ethylene oxide). Nano Lett 16(1):459–465
68. Li S, Zhang SQ, Shen L, Liu Q, Ma JB, Lv W, He YB, Yang QH (2020) Progress and perspective of ceramic/polymer composite solid electrolytes for lithium batteries. Adv Sci 7(5):1903088
69. Wang L, Wu Z, Zou J, Gao P, Niu X, Li H, Chen L (2019) Li-free cathode materials for high energy density lithium batteries. Joule 3(9):2086–2102
70. Dey A, Karan S, De SK (2013) Effect of nano additives on ionic conductivity of solid polymer electrolyte. 51(05):281–288
71. Wu M, Song J, Zhu X, Zhan H, Tian T, Wang R, Lei J, Tang H (2023) Three-dimensional hierarchical composite polymer electrolyte with enhanced interfacial compatibility for all-solid-state lithium metal batteries. Sci China Mater 66(2):522–530
72. Shi Y, Li B, Zhu Q, Shen K, Tang W, Xiang Q, Chen W, Liu C, Luo J, Yang S (2020) MXene-based mesoporous nanosheets toward superior lithium-ion conductors. Adv Energy Mater 10(9):1903534
73. Aravindan V, Gnanaraj J, Madhavi S, Liu HK (2011) Lithium-ion conducting electrolyte salts for lithium batteries. Chem Eur J 17(51):14326–14346
74. Xia S, Wu X, Zhang Z, Cui Y, Liu W (2019) Practical challenges and future perspectives of all-solid-state lithium-metal batteries. Chem 5(4):753–785
75. Gauthier M, Carney TJ, Grimaud A, Giordano L, Pour N, Chang HH, Fenning DP, Lux SF, Paschos O, Bauer C, Maglia F (2015) Electrode–electrolyte interface in Li-ion batteries:

current understanding and new insights. J Phys Chem Lett 6(22):4653–4672

76. Pan Q, Barbash D, Smith DM, Qi H, Gleeson SE, Li CY (2017) Correlating electrode–electrolyte interface and battery performance in hybrid solid polymer electrolyte-based lithium metal batteries. Adv Energy Mater 7(22):1701231
77. Duan H, Fan M, Chen WP, Li JY, Wang PF, Wang WP, Shi JL, Yin YX, Wan LJ, Guo YG (2019) Extended electrochemical window of solid electrolytes via heterogeneous multilayered structure for high-voltage lithium metal batteries. Adv Mater 31(12):1807789
78. Shi Y, Wan J, Liu GX, Zuo TT, Song YX, Liu B, Guo YG, Wen R, Wan LJ (2022) Interfacial evolution of lithium dendrites and their solid electrolyte interphase shells of quasi-solid-state lithium-metal batteries. Angew Chem Int Ed 59(41):18120–18255
79. Ibrahim S, Yassin MM, Ahmad R, Johan MR (2011) Effects of various LiPF 6 salt concentrations on PEO-based solid polymer electrolytes. Ionics 399-405
80. Zhou W, Wang Z, Pu Y, Li Y, Xin S, Li X, Chen J, Goodenough JB (2019) Double-layer polymer electrolyte for high-voltage all-solid-state rechargeable batteries. Adv Mater 31(4):1805574
81. Barbosa PC, Rodrigues LC, Silva MM, Smith MJ (2011) Characterization of pTMCnLiPF6 solid polymer electrolytes. Solid State Ion 193(1):39–42
82. Varishetty MM, Qiu W, Gao Y, Chen W (2010) Structure, electrical and optical properties of (PVA/LiAsF6) polymer composite electrolyte films. Polym Eng Sci 50(5):878–884
83. Itoh T, Nakamura K, Uno T, Kubo M (2018) Thermal and electrochemical properties of poly (2, 2-dimethoxypropylene carbonate)-based solid polymer electrolyte for polymer battery. Solid State Ion 317:69–75
84. Appetecchi GB, Zane D, Scrosati B (2004) PEO-based electrolyte membranes based on LiBC4 O 8 Salt. J Electrochem Soc 151(9):A1369
85. Chong WG, Osman Z (2014) The effect of carbonate-phthalate plasticizers on structural, morphological, and electrical properties of polyacrylonitrile-based solid polymer electrolytes. J Polymer Res 21:1–9
86. Tao SD, Li J, Hu R, Wang L, Chi Z (2021) Li T. 3Li2S-2MoS2 filled composite polymer PVDF-HFP/LiODFB electrolyte with excellent interface performance for lithium metal batteries. Appl Surf Sci 536:147794
87. Feng J, Wang L, Chen Y, Wang P, Zhang H, He X (2021) PEO-based polymer-ceramic hybrid solid electrolytes: a review. Nano Converg 8:1–2
88. Jiang K, Wang J, Zuo C, Li S, Li S, He D, Peng H, Xie X, Poli R, Xue Z (2020) Facile fabrication of polymer electrolytes via lithium salt-accelerated thiol-michael addition for lithium-ion batteries. Macromolecules 53(17):7450–7459
89. Wang C, Fu K, Kammampata SP, McOwen DW, Samson AJ, Zhang L, Hitz GT, Nolan AM, Wachsman ED, Mo Y, Thangadurai V (2020) Garnet-type solid-state electrolytes: materials, interfaces, and batteries. Chem Rev 120(10):4257–4300
90. Bashiri P, Rao TP, Naik VM, Nazri GA, Naik R (2019) AC conductivity studies of polyethylene oxide-garnet-type Li7La3Zr2O12 hybrid composite solid polymer electrolyte films. Solid State Ion 343:115089
91. Li L, Deng Y, Chen G (2020) Status and prospect of garnet/polymer solid composite electrolytes for all-solid-state lithium batteries. J Energy Chem 50:154–177
92. Gao Y, Sun S, Zhang X, Liu Y, Hu J, Huang Z, Gao M, Pan H (2021) Amorphous dual-layer coating: enabling high Li-ion conductivity of non-sintered garnet-type solid electrolyte. Adv Funct Mater 31(15):2009692
93. Yang T, Zheng J, Cheng Q, Hu YY, Chan CK (2017) Composite polymer electrolytes with Li7La3Zr2O12 garnet-type nanowires as ceramic fillers: mechanism of conductivity enhancement and role of doping and morphology. ACS Appl Mater Interfaces 9(26):21773–21780
94. Qin Z, Meng X, Xie Y, Qian D, Deng H, Mao D, Wan L, Huang Y (2021) Fast Li-ion transport pathways via 3D continuous networks in homogeneous garnet-type electrolyte for solid-state lithium batteries. Energy Stor Mater 43:190–201
95. Yi M, Liu T, Li J, Wang C, Mo Y, Wang X, Wei Y (2019) High Li-ion conductivity of Al-free Li 7-3 x Ga x La 3 Zr 2 O 12 solid electrolyte prepared by liquid-phase sintering. J Solid State Electrochem 23:1249–1256
96. Yu S, Schmidt RD, Garcia-Mendez R, Herbert E, Dudney NJ, Wolfenstine JB, Sakamoto J, Siegel DJ (2016) Elastic properties of the solid electrolyte Li7La3Zr2O12 (LLZO). Chem Mater 28(1):197–206
97. Li R, Guo S, Yu L, Wang L, Wu D, Li Y, Hu X (2019) Morphosynthesis of 3D macroporous garnet frameworks and perfusion of polymer-stabilized lithium salts for flexible solid-state hybrid electrolytes. Adv Mater Interfaces 6(10):1900200
98. Bae J, Li Y, Zhao F, Zhou X, Ding Y, Yu G (2018) Designing 3D nanostructured garnet frameworks for enhancing ionic conductivity and flexibility in composite polymer electrolytes for lithium batteries. Energy Stor Mater 15:46–52
99. Wang X, Hao X, Xia Y, Liang Y, Xia X, Tu J (2019) A polyacrylonitrile (PAN)-based double-layer multifunctional gel polymer electrolyte for lithium-sulfur batteries. J Membr Sci 582:37–47
100. Xu H, Zhang X, Jiang J, Li M, Shen Y (2020) Ultrathin Li7La3Zr2O12@ PAN composite polymer electrolyte with high conductivity for all-solid-state lithium-ion battery. Solid State Ion 347:115227
101. Gao L, Li J, Ju J, Cheng B, Kang W, Deng N (2020) Polyvinylidene fluoride nanofibers with embedded Li6. 4La3Zr1. 4Ta0. 6O12 fillers modified polymer electrolytes for high-capacity and long-life all-solid-state lithium metal batteries. Compos Sci Technol 200:108408
102. He K, Chen C, Fan R, Liu C, Liao C, Xu Y, Tang J, Li RK (2019) Polyethylene oxide/garnet-type Li6. 4La3Zr1. 4Nb0. 6O12 composite electrolytes with improved electrochemical performance for solid-state lithium rechargeable batteries. Compos Sci Technol 175:28–34
103. Song S, Wu Y, Tang W, Deng F, Yao J, Liu Z, Hu R, Alamusi WZ, Lu L, Hu N (2019) Composite solid polymer electrolyte with garnet nanosheets in poly (ethylene oxide). ACS Sustain Chem Eng 7(7):7163–7170
104. Xie Z, Wu Z, An X, Yue X, Xiaokaiti P, Yoshida A, Abudula A, Guan G (2020) A sandwich-type composite polymer electrolyte for all-solid-state lithium metal batteries with high areal capacity and cycling stability. J Membr Sci 596:117739
105. Song S, Qin X, Ruan Y, Li W, Xu Y, Zhang D, Thokchom J (2020) Enhanced performance of solid-state lithium-air batteries with continuous 3D garnet network added composite polymer electrolyte. J Power Sources 461:228146
106. Jiang T, He P, Wang G, Shen Y, Nan CW, Fan LZ (2020) Solvent-free synthesis of thin, flexible, nonflammable garnet-based composite solid electrolyte for all-solid-state lithium batteries. Adv Energy Mater 10(12):1903376
107. Zhang J, Zhao N, Zhang M, Li Y, Chu PK, Guo X, Di Z, Wang X, Li H (2016) Flexible and ion-conducting membrane electrolytes for solid-state lithium batteries: dispersion of garnet nanoparticles in insulating polyethylene oxide. Nano Energy 28:447–454
108. Choi JH, Lee CH, Yu JH, Doh CH, Lee SM (2015) Enhancement of ionic conductivity of composite membranes for all-solid-state lithium rechargeable batteries incorporating tetragonal Li7La3Zr2O12 into a polyethylene oxide matrix. J Power Sources 274:458–463
109. Zha W, Chen F, Yang D, Shen Q, Zhang L (2018) High-performance Li6. 4La3Zr1. 4Ta0. 6O12/Poly (ethylene oxide)/

Succinonitrile composite electrolyte for solid-state lithium batteries. J Power Sources 397:87–94

110. Cheng SH, He KQ, Liu Y, Zha JW, Kamruzzaman M, Ma RL, Dang ZM, Li RK, Chung CY Electrochemical performance of all-solid-state lithium batteries using inorganic lithium garnets particulate reinforced PEO/LiClO4 electrolyte. Electrochim Acta 253:430–438
111. Xia Y, Wang X, Xia X, Xu R, Zhang S, Wu J, Liang Y, Gu C, Tu J (2017) A newly designed composite gel polymer electrolyte based on poly (vinylidene fluoride-hexafluoropropylene) (PVDF-HFP) for enhanced solid-state lithium-sulfur batteries. Chem Eur J 23(60):15203–15209
112. Le HT, Ngo DT, Kalubarme RS, Cao G, Park CN, Park CJ (2016) Composite gel polymer electrolyte based on poly (vinylidene fluoride-hexafluoropropylene) (PVDF-HFP) with modified aluminum-doped lithium lanthanum titanate (A-LLTO) for high-performance lithium rechargeable batteries. ACS Appl Mater Interfaces 8(32):20710–20719
113. Deng Y, Eames C, Nguyen LH, Pecher O, Griffith KJ, Courty M, Fleutot B, Chotard JN, Grey CP, Islam MS, Masquelier C (2018) Crystal structures, local atomic environments, and ion diffusion mechanisms of scandium-substituted sodium superionic conductor (NASICON) solid electrolytes. Chem Mater 30(8):2618–2630
114. Kothari DH, Kanchan DK (2022) Inter-grain Li+ conduction in Sc and Y doped LATP compounds. Phys B Condens 627:413599
115. Kou Z, Miao C, Wang Z, Mei P, Zhang Y, Yan X, Jiang Y, Xiao W (2019) Enhanced ionic conductivity of novel composite polymer electrolytes with Li1. 3Al0. 3Ti1. 7 (PO4) 3 NASICON-type fast ion conductor powders. Solid State Ion 338:138–143
116. Yang J, Huang Z, Zhang P, Liu G, Xu X, Yao X (2019) Titanium dioxide doping toward high-lithium-ion-conducting Li1. 5Al0. 5Ge1. 5 (PO4) 3 glass-ceramics for all-solid-state lithium batteries. ACS Appl Energy Mater 2(10):7299–7305
117. Jin Y, Liu C, Zong X, Li D, Fu M, Tan S, Xiong Y, Wei J (2020) Interface engineering of Li1. 3Al0. 3Ti1. 7 (PO4) 3 ceramic electrolytes via multifunctional interfacial layer for all-solid-state lithium batteries. J Power Sources 460:228125
118. Kou Z, Miao C, Wang Z, Xiao W (2019) Novel NASICON-type structural Li1. 3Al0. 3Ti1. 7SixP5 (3-0.8 x) O12 solid electrolytes with improved ionic conductivity for lithium-ion batteries. Solid State Ionics 343:115090
119. Zhao E, Guo Y, Xin Y, Xu G, Guo X (2020) Enhanced electrochemical properties and interfacial stability of poly (ethylene oxide) solid electrolyte incorporating nanostructured Li1. 3Al0. 3Ti1. 7 (PO4) 3 fillers for all-solid-state lithium-ion batteries. Int J Energy Res 45(5):6876–6887
120. Dong GH, Mao YQ, Yang GM, Li YQ, Song SF, Xu CH, Huang P, Hu N, Fu SY (2021) High-strength poly (ethylene oxide) composite electrolyte reinforced with glass fiber and ceramic electrolyte simultaneously for structural energy storage. ACS Appl Energy Mater 4(4):4038–4049
121. Bonizzoni S, Ferrara C, Berbenni V, Anselmi-Tamburini U, Mustarelli P, Tealdi C (2019) NASICON-type polymer-in-ceramic composite electrolytes for lithium batteries. Phys Chem Chem Phys 21(11):6142–6149
122. Wang X, Hao X, Xia Y, Liang Y, Xia X, Tu J (2019) A polyacrylonitrile (PAN)-based double-layer multifunctional gel polymer electrolyte for lithium-sulfur batteries. J Membr Sci 582:37–47
123. Liu L, Chu L, Jiang B, Li M (2019) Li1. 4Al0. 4Ti1. 6 (PO4) 3 nanoparticle-reinforced solid polymer electrolytes for all-solid-state lithium batteries. Solid State Ion 331:89–95
124. Yu X, Li J, Manthiram A (2020) Rational design of a laminated dual-polymer/polymer–ceramic composite electrolyte for high-voltage all-solid-state lithium batteries. ACS Mater Lett 2(4):317–324
125. Aliahmad N, Shrestha S, Varahramyan K, Agarwal M (2016) Poly (vinylidene fluoride-hexafluoropropylene) polymer electrolyte for paper-based and flexible battery applications. AIP Adv 6(6):065206
126. Pareek T, Dwivedi S, Ahmad SA, Badole M, Kumar S (2020) Effect of NASICON-type LiSnZr (PO4) 3 ceramic filler on the ionic conductivity and electrochemical behavior of PVDF based composite electrolyte. J Alloys Compd 824:153991
127. Zhou Q, Li Q, Liu S, Yin X, Huang B, Sheng M (2021) High Li-ion conductive composite polymer electrolytes for all-solid-state Li-metal batteries. J Power Sources 482:228929
128. Wang W, Yi E, Fici AJ, Laine RM, Kieffer J (2017) Lithium-ion conducting poly (ethylene oxide)-based solid electrolytes containing active or passive ceramic nanoparticles. J Phys Chem C 121(5):2563–2573
129. Siyal SH, Shah SS, Najam T, Javed MS, Imran M, Lan JL (2021) Significant reduction in interface resistance and super-enhanced performance of the lithium-metal battery by in situ construction of poly (vinylidene fluoride)-based solid-state membrane with dual ceramic fillers. ACS Appl Energy Mater 4(8):8604–8614
130. Huang Y, Zhang Z, Gao H, Huang J, Li C (2020) Li1. 5Al0. 5Ti1. 5 (PO4) 3 enhanced polyethylene oxide polymer electrolyte for all-solid-state lithium batteries. Solid State Ion 356:115437
131. Chen SY, Hsieh CT, Zhang RS, Mohanty D, Gandomi YA, Hung IM (2022) Hybrid solid-state electrolytes blending NASICON-type Li1+ xAlxTi2–x (PO4) 3 with poly (vinylidene fluoride-co-hexafluoropropylene) for lithium metal batteries. Electrochim Acta 427:140903
132. Yang S, Zhang Z, Shen L, Chen P, Gu Z, Chang M, He H, Yao X (2022) Gravity-driven Poly (ethylene glycol) @ Li1. 5Al0. 5Ge1. 5 (PO4) 3 asymmetric solid polymer electrolytes for all-solid-state lithium batteries. J Power Sources 518:230756
133. Sung BJ, Didwal PN, Verma R, Nguyen AG, Chang DR, Park CJ (2021) Composite solid electrolyte comprising poly (propylene carbonate) and Li1. 5Al0. 5Ge1. 5 (PO4) 3 for long-life all-solid-state Li-ion batteries. Electrochim Acta 392:139007
134. Zhai L, Zhang W, Gong H, Li Y, Gao M, Zhang X, Li D, Zhou Y, Dong C, Liu W, Jiang F (2022) Quasi-solid polymer electrolytes with fast interfacial transport for lithium metal batteries. Surf Interfaces 34:102299
135. Piana G, Bella F, Geobaldo F, Meligrana G, Gerbaldi C (2019) PEO/LAGP hybrid solid polymer electrolytes for ambient temperature lithium batteries by solvent-free,"one pot" preparation. J Energy Stor 26:100947
136. Jin Y, Liu C, Jia Z, Zong X, Li D, Fu M, Wei J, Xiong Y (2021) Building a highly functional Li1. 3Al0. 3Ti1. 7 (PO4) 3/poly (vinylidene fluoride) composite electrolyte for all-solid-state lithium batteries. J Alloys Compd 874:159890
137. Zhao W, Yi J, He P, Zhou H (2019) Solid-state electrolytes for lithium-ion batteries: fundamentals, challenges and perspectives. Electrochem Energy Rev 2:574–605
138. Choi HJ, Kim SY, Gong MK, Vignesh H, Aravindan V, Lee YG, Lee YS (2017) Tailored perovskite Li0. 33La0. 56TiO3 via an adipic acid-assisted solution process: a promising solid electrolyte for lithium batteries. J Alloys Compd 729:338–343
139. Bohnke O, Bohnke C, Fourquet JL (1996) Mechanism of ionic conduction and electrochemical intercalation of lithium into the perovskite lanthanum lithium titanate. Solid State Ion 91(1-2):21–31
140. Sun LL, Li YF, Li G, Wang LG, Tong YY (2019) Perovskite-type compounds in anion-substituted LiSr1− 0.5 xTiTaO6− xFx electrolyte for improving lithium-ion conduction. Ceram Int 45(2):2381–2384
141. Li R, Liao K, Zhou W, Li X, Meng D, Cai R, Shao Z (2019) Realizing fourfold enhancement in conductivity of perovskite

Li0. 33La0. 557TiO3 electrolyte membrane via a Sr and Ta co-doping strategy. J Membr Sci 582:194–202

142. Zhu P, Yan C, Dirican M, Zhu J, Zang J, Selvan RK, Chung CC, Jia H, Li Y, Kiyak Y, Wu N (2018) Li 0.33 La 0.557 TiO 3 ceramic nanofiber-enhanced polyethylene oxide-based composite polymer electrolytes for all-solid-state lithium batteries. J Mater Chem A 6(10):4279–4285
143. Sun C, Alonso JA, Bian J (2021) Recent advances in perovskite-type oxides for energy conversion and storage applications. Adv Energy Mater 11(2):2000459
144. Sengodan S, Yeo HJ, Shin JY, Kim G (2011) Assessment of perovskite-type La0. 8Sr0. 2ScxMn1− xO3–δ oxides as anodes for intermediate-temperature solid oxide fuel cells using hydrocarbon fuels. J Power Sources 196(6):3083–3088
145. He KQ, Zha JW, Du P, Cheng SH, Liu C, Dang ZM, Li RK (2019) Tailored high cycling performance in a solid polymer electrolyte with perovskite-type Li 0.33 La 0.557 TiO 3 nanofibers for all-solid-state lithium-ion batteries. Dalton Trans 48(10):3263–3269
146. Wei W, Li L, Zhang L, Hong J, He G (2018) An all-solid-state Li-organic battery with quinone-based polymer cathode and composite polymer electrolyte. Electrochem Commun 90:21–25
147. Pila CR, Cappe EP, Mohallem ND, Alves OL, Frutis MA, Sánchez-Ramírez N, Torresi RM, Ramírez HL, Laffita YM (2019) Effect of the LLTO nanoparticles on the conducting properties of PEO-based solid electrolyte. Solid State Sci 88:41–47
148. Zhu L, Zhu P, Fang Q, Jing M, Shen X, Yang L (2018) A novel solid PEO/LLTO-nanowires polymer composite electrolyte for solid-state lithium-ion battery. Electrochim Acta 292:718–726
149. Wang W, Lin B, Zhang H, Sun Y, Zhang X, Yang H (2019) Synthesis, morphology and electrochemical performances of perovskite-type oxide LaxSr1-xFeO3 nanofibers prepared by electrospinning. J Phys Chem Solid 124:144–150
150. Yang TQ, Wang C, Zhang WK, Xia Y, Gan YP, Huang H, He XP, Zhang J (2022) Composite polymer electrolytes reinforced by a three-dimensional polyacrylonitrile/Li0. 33La0. 557TiO3 nanofiber framework for room-temperature dendrite-free all-solid-state lithium metal battery. Rare Met 41(6):1870–1879
151. He K, Cheng SH, Hu J, Zhang Y, Yang H, Liu Y, Liao W, Chen D, Liao C, Cheng X, Lu Z (2021) In-situ intermolecular interaction in composite polymer electrolyte for ultralong life quasi-solid-state lithium metal batteries. Angew Chem Int Ed 60(21):12116–12123
152. Wang C, Zhang XW, Appleby AJ (2004) Solvent-free composite PEO-ceramic fiber/mat electrolytes for lithium secondary cells. J Electrochem Soc 152(1):A205
153. Chen S, Xie D, Liu G, Mwizerwa JP, Zhang Q, Zhao Y, Xu X, Yao X (2018) Sulfide solid electrolytes for all-solid-state lithium batteries: structure, conductivity, stability and application. Energy Stor Mater 14:58–74
154. Bai Y, Zhao Y, Li W, Meng L, Bai Y, Chen G (2020) Organic-inorganic multi-scale enhanced interfacial engineering of sulfide solid electrolyte in Li-S battery. Chem Eng J 396:125334
155. Wang S, Zhang X, Liu S, Xin C, Xue C, Richter F, Li L, Fan L, Lin Y, Shen Y, Janek J (2020) High-conductivity free-standing Li6PS5Cl/poly (vinylidene difluoride) composite solid electrolyte membranes for lithium-ion batteries. J Mater 6(1):70–76
156. Palmer MJ, Kalnaus S, Dixit MB, Westover AS, Hatzell KB, Dudney NJ, Chen XC (2020) A three-dimensional interconnected polymer/ceramic composite as a thin film solid electrolyte. Energy Stor Mater 26:242–249
157. Li Y, Arnold W, Thapa A, Jasinski JB, Sumanasekera G, Sunkara M, Druffel T, Wang H (2020) Stable and flexible sulfide composite electrolyte for high-performance solid-state lithium batteries. ACS Appl Mater Interfaces 12(38):42653–42659
158. Lai C, Shu C, Li W, Wang L, Wang X, Zhang T, Yin X, Ahmad I, Li M, Tian X, Yang P (2020) Stabilizing a lithium metal battery by an in situ Li2S-modified interfacial layer via amorphous-sulfide composite solid electrolyte. Nano Lett 20(11):8273–8281
159. Li M, Kolek M, Frerichs JE, Sun W, Hou X, Hansen MR, Winter M, Bieker P (2021) Investigation of polymer/ceramic composite solid electrolyte system: the case of PEO/LGPS composite electrolytes. ACS Sustain Chem Eng 9(34):11314–11322
160. Zhao Y, Wu C, Peng G, Chen X, Yao X, Bai Y, Wu F, Chen S, Xu X (2016) A new solid polymer electrolyte incorporating Li10GeP2S12 into a polyethylene oxide matrix for all-solid-state lithium batteries. J Power Sources 301:47–53
161. Ma Z, Xue HG, Guo SP (2018) Recent achievements on sulfide-type solid electrolytes: crystal structures and electrochemical performance. J Mater Sci 53(6):3927–3393
162. Zhang D, Xu X, Qin Y, Ji S, Huo Y, Wang Z, Liu Z, Shen J, Liu J (2020) Recent progress in organic–inorganic composite solid electrolytes for all-solid-state lithium batteries. Chem Eur J 26(8):1720–1736
163. Chen B, Huang Z, Chen X, Zhao Y, Xu Q, Long P, Chen S, Xu X (2016) A new composite solid electrolyte PEO/Li10GeP2S12/SN for an all-solid-state lithium battery. Electrochim Acta 210:905–914
164. Chen S, Wang J, Zhang Z, Wu L, Yao L, Wei Z, Deng Y, Xie D, Yao X, Xu X (2018) In-situ preparation of poly (ethylene oxide)/Li3PS4 hybrid polymer electrolyte with good nanofiller distribution for rechargeable solid-state lithium batteries. J Power Sources 387:72–80
165. Li X, Wang D, Wang H, Yan H, Gong Z, Yang Y (2019) Poly (ethylene oxide)–Li10SnP2S12 composite polymer electrolyte enables high-performance all-solid-state lithium-sulfur battery. ACS Appl Mater Interfaces 11(25):22745–22753
166. Liu Q, Jiang L, Zheng P, Sun J, Liu C, Chai J, Li X, Zheng Y, Liu Z (2022) Recent advances in stability issues of inorganic solid electrolytes and composite solid electrolytes for all-solid-state batteries. Chem Rec 22(10):e202200116
167. Ahmed SA, Pareek T, Dwivedi S, Badole M, Kumar S (2020) LiSn 2 (PO 4) 3-based polymer-in-ceramic composite electrolyte with high ionic conductivity for all-solid-state lithium batteries. J Solid State Electrochem 24:2407–2417
168. Dhatarwal P, Choudhary S, Sengwa RJ (2018) Electrochemical performance of Li+-ion conducting solid polymer electrolytes based on PEO–PMMA blend matrix incorporated with various inorganic nanoparticles for the lithium-ion batteries. Compos Commun 10:11–17
169. Singh P, Saroj AL (2021) Effect of SiO2 Nano-particles on plasticized polymer blend electrolytes: vibrational, thermal, and ionic conductivity study. Polym Plast Technol Mater 60(3):298–305
170. Jagan M, Vijayachamundeeswari SP (2023) A comprehensive investigation of lithium-based polymer electrolytes. J Polymer Res 30(6):250
171. Lyu W, He G, Liu T (2020) PEO-LITFSI-SiO2-SN system promotes the application of polymer electrolytes in all-solid-state lithium-ion batteries. ChemistryOpen 9(6):713–718
172. Yanilmaz M (2020) Evaluation of electrospun PVA/SiO2 nanofiber separator membranes for lithium-ion batteries. J Text Inst 111(3):447–452
173. Pal P, Ghosh A (2018) Influence of TiO2 nano-particles on charge carrier transport and cell performance of PMMA-LiClO4 based nano-composite electrolytes. Electrochim Acta 260:157–167
174. Vickraman P, Reddy BJ (2019) Performance of ferroceramic PVDF-co-HEP micro composite electrolytes cum separators for Li-ion batteries. AIP Conf Proc 2115(1):030533

175. Hema M, Tamilselvi P (2016) Lithium-ion conducting PVA: PVdF polymer electrolytes doped with nano SiO2 and TiO2 filler. J Phys Chem Solid 96:42–48
176. Chen HC, Lin FJ, Chen CC (2002) Polyacrylonitrile electrolytes 1. A novel high-conductivity composite polymer electrolyte based on PAN, LiClO 4, and a-Al 2 O 3. Solid State Ion 50:327–335
177. Liang B, Tang S, Jiang Q, Chen C, Chen X, Li S, Yan X (2015) Preparation and characterization of PEO-PMMA polymer composite electrolytes doped with nano-Al2O3. Electrochim Acta 169:334–341
178. Vijayakumar G, Karthick SN, Subramania A (2011) A new class of P (VdF-HFP)-CeO2-LiClO4-based composite microporous membrane electrolytes for Li-ion batteries. Int J Electrochem
179. Chen H, Adekoya D, Hencz L, Ma J, Chen S, Yan C, Zhao H, Cui G, Zhang S (2020) Stable seamless interfaces and rapid ionic conductivity of Ca–CeO2/LiTFSI/PEO composite electrolyte for high-rate and high-voltage all-solid-state battery. Adv Energy Mater 10(21):2000049
180. Sharma J, Hashmi S (2019) Magnesium ion-conducting gel polymer electrolyte nanocomposites: Effect of active and passive nanofillers. Polym Compos 40(4):1295–1306
181. Vijayakumar G, Karthick SN, Paramasivam R, Ilamaran C (2012) Morphology and electrochemical properties of P (VdF-HFP)/MgO-based composite microporous polymer electrolytes for Li-ion polymer batteries. Polym-Plast Technol Eng 51(14):1427–1431
182. Premila R, Subbu C, Rajendran SJ (2018) Experimental investigation of nano filler TiO2 doped composite polymer electrolytes for lithium-ion batteries. Appl Surf Sci 449:426–434
183. He Z, Cao Q, Jing B, Wang X, Deng Y (2017) Gel electrolytes based on poly (vinylidene fluoride-co-hexafluoropropylene)/thermoplastic polyurethane/poly (methyl methacrylate) with in situ SiO 2 for polymer lithium batteries. RSC Adv 7(6):3240–3248
184. Lee L, Park SJ, Kim S (2013) Effect of nano-sized barium titanate addition on PEO/PVDF blend-based composite polymer electrolytes. Solid State Ion 234:19–24
185. Zhang Z, Wang Q, Li Z, Jiang Y, Zhao B, Han X (2019) Well-aligned BaTiO3 nanofibers via solution blow spinning and their application in lithium composite solid-state electrolyte. Mater Express 9(9):993–1000
186. Kumar R, Subramania A, Sundaram NK, Kumar GV, Baskaran I (2007) Effect of MgO nanoparticles on ionic conductivity and electrochemical properties of nanocomposite polymer electrolyte. J Membr Sci 300(1-2):104–110
187. Yu X, Manthiram A (2021) A review of composite polymer-ceramic electrolytes for lithium batteries. Energy Stor Mater 34:282–300
188. Sasikumar M, Raja M, Krishna RH, Jagadeesan A, Sivakumar P, Rajendran S (2018) Influence of hydrothermally synthesized cubic-structured BaTiO3 ceramic fillers on ionic conductivity, mechanical integrity, and thermal behavior of P (VDF–HFP)/PVAc-based composite solid polymer electrolytes for lithium-ion batteries. J Phys Chem C 122(45):25741–25752
189. Hu J, Wang W, Zhou B, Feng Y, Xie X, Xue Z (2019) Poly (ethylene oxide)-based composite polymer electrolytes embedding with ionic bond modified nanoparticles for all-solid-state lithium-ion battery. J Membr Sci 575:200–208
190. Rao MM, Liu JS, Li WS, Liao YH, Liang Y, Zhao LZ (2010) Polyethylene-supported poly (acrylonitrile-co-methyl methacrylate)/nano-Al$_2$O$_3$ microporous composite polymer electrolyte for lithium-ion battery. J Solid State Electrochem 14:255–261
191. Arya A, Sharma AL (2018) Optimization of salt concentration and explanation of two peak percolation in blend solid polymer nanocomposite films. J Solid State Electrochem 22:2725–2745
192. Karuppasamy K, Antony R, Alwin S, Balakumar S, Sahaya Shajan X (2015) A review on PEO-based solid polymer electrolytes (SPEs) complexed with LiX (X= Tf, BOB) for rechargeable lithium-ion batteries. Mater Sci 807:41–63
193. Pavlidou S, Papaspyrides CD (2008) A review on polymer–layered silicate nanocomposites. Prog Polym Sci 33(12):1119–1198
194. Erceg M, Jozić D, Banovac I, Perinović S, Bernstorff S (2014) Preparation and characterization of melt intercalated poly (ethylene oxide)/lithium montmorillonite nanocomposites. Thermochem Acta 579:86–92
195. Park CH, Park M, Yoo SI, Joo SK (2006) A spin-coated solid polymer electrolyte for all-solid-state rechargeable thin-film lithium polymer batteries. J Power Sources 158(2):1442–1446
196. Patel G, Sureshkumar MB (2014) Preparation of PAM/PVA blending films by solution-cast technique and its characterization: a spectroscopic study. Iran Polym J 23:153–162
197. Ahmed F, Kumar S, Arshi N, Anwar MS, Su-Yeon L, Kil GS, Park DW, Koo BH, Lee CG (2011) Preparation and characterizations of polyaniline (PANI)/ZnO nanocomposites film using solution casting method. Thin Solid Films 519(23):8375–8378
198. Krebs FC (2009) Fabrication and processing of polymer solar cells: a review of printing and coating techniques. Sol Energy Mater Sol Cells 93(4):394–412
199. Barick AK, Tripathy DK (2011) Preparation and characterization of thermoplastic polyurethane/organoclay nanocomposites by melt intercalation technique: effect of nano clay on morphology, mechanical, thermal, and rheological properties. J Appl Polym Sci 117(2):639–654
200. Tyona MD (2013) A theoritical study on spin coating technique. Adv Mat Res 2(4):195
201. Bordes P, Pollet E, Bourbigot S, Averous L (2008) Structure and properties of PHA/clay nano-bio composites prepared by melt intercalation. Macromol Chem Phys 209(14):1473–1484
202. Wilson MS, Gottesfeld S (1992) Thin-film catalyst layers for polymer electrolyte fuel cell electrodes. J Appl Electrochem 22(1):1–7
203. Agrawal RC, Chandra A (2007) Ion transport and electrochemical cell performance studies on hot press-synthesized Ag+ ion conducting electroactive polymeric membranes:(1− x) PEO: x [0.7 (0.75 AgI: 0.25 AgCl): 0.3 MI]. J Phys D Appl Phys 40(22):7024
204. Brinker CJ, Hurd AJ (1994) Fundamentals of sol-gel dip-coating. J Phys III 4(7):1231–1242
205. Birnie III DP. (2004) Spin coating technique. Sol-gel technologies for glass producers and users. 49-55.
206. Firdaus CM, Rizam MS, Rusop M, Hidayah SR (2012) Characterization of ZnO and ZnO: TiO2 thin films prepared by sol-gel spray-spin coating technique. Procedia Eng 41:1367–1373
207. Puetz J, Aegerter MA (2004) Dip coating technique. Sol Gel Technol Glass Prod Users:37–48
208. Brinker CJ (2013) Dip coating. In: chemical solution deposition of functional oxide thin films. Springer Vienna, Vienna, pp 233–261